Apoptosis (2015) 20:996–1015
DOI 10.1007/s10495-015-1131-3

ORIGINAL PAPER

Regulation of viability, differentiation and death of human melanoma cells carrying neural stem cell biomarkers: a possibility for neural trans-differentiation

Vladimir N. Ivanov[1] · **Tom K. Hei**[1]

Published online: 8 May 2015

Abstract During embryonic development, melanoblasts, the precursors of melanocytes, emerge from a subpopulation of the neural crest stem cells and migrate to colonize skin. Melanomas arise during melanoblast differentiation into melanocytes and from young proliferating melanocytes through somatic mutagenesis and epigenetic regulations. In the present study, we used several human melanoma cell lines from the sequential phases of melanoma development (radial growth phase, vertical growth phase and metastatic phase) to compare: (i) the frequency and efficiency of the induction of cell death via apoptosis and necroptosis; (ii) the presence of neural and cancer stem cell biomarkers as well as death receptors, DR5 and FAS, in both adherent and spheroid cultures of melanoma cells; (iii) anti-apoptotic effects of the endogenous production of cytokines and (iv) the ability of melanoma cells to perform neural trans-differentiation. We demonstrated that programed necrosis or necroptosis, could be induced in two metastatic melanoma lines, FEMX and OM431, while the mitochondrial pathway of apoptosis was prevalent in a vast majority of melanoma lines. All melanoma lines used in the current study expressed substantial levels of pluripotency markers, SOX2 and NANOG. There was a trend for increasing expression of Nestin, an early neuroprogenitor marker, during melanoma progression. Most of the melanoma lines, including WM35, FEMX and A375, can grow as a spheroid culture in serum-free media with supplements. It was possible to induce neural trans-differentiation of 1205Lu and OM431 melanoma cells in serum-free media supplemented with insulin. This was confirmed by the expression of neuronal markers, doublecortin and β3-Tubulin, by significant growth of neurites and by the negative regulation of this process by a dominant-negative Rac1N17. These results suggest a relative plasticity of differentiated melanoma cells and a possibility for their neural trans-differentiation without the necessity for preliminary dedifferentiation.

Keywords Melanoma · Apoptosis · Necroptosis · Neural stem cells · Transdifferentiation

Abbreviations

EGF	Epidermal growth factor
ERK1/2	Extracellular-signal-regulated kinases
FACS	Fluorescence-activated cell sorter
FGF2	Fibroblast growth factor-2 (basic)
IκB	Inhibitor of NF-κB
IKK	Inhibitor nuclear factor kappa B kinase
JNK	C-Jun N-terminal kinase
MAPK	Mitogen-activated protein kinase
MEK	MAPK/ERK kinase
NF-κB	Nuclear factor kappa B
NSC	Neural stem cells
PARP-1	Poly (ADP-ribose) polymerase-1
PI	Propidium iodide
PI3K	Phosphoinositide 3-kinase
STAT	Signal transducers and activators of transcription
TNFα	Tumor necrosis factor

Electronic supplementary material The online version of this article (doi:10.1007/s10495-015-1131-3) contains supplementary material, which is available to authorized users.

✉ Vladimir N. Ivanov
vni3@cumc.columbia.edu

[1] Center for Radiological Research, Department of Radiation Oncology, College of Physicians and Surgeons, Columbia University, 630 West 168th Street, New York, NY 10032, USA

zVAD Carbobenzoxy-valyl-alanyl-aspartyl-[*O*-methyl]-fluoromethylketone

Introduction

Significant progress has been made during the last 15 years in new molecule targeted therapies for treatment of advanced cancers, including melanomas. There are several dominant genetic alterations during melanoma carcinogenesis: (i) *BRAF* and *NRAS* gene mutations [1–3], which were found in nearly 50–60 and 20 % of melanomas, respectively; (ii) deletion of the *CDKN2A* locus, which encoded two tumor suppressor proteins, $p16^{INK4a}$ and $p14^{ARF}$, was found in up to 50 % of melanomas [4]; (iii) deletion or mutation of PTEN, an endogenous inhibitor of PI3K-AKT, was found in 20 % of melanomas [5]; (iv) finally, mutations of *TP53* were found in 19 % of melanomas [6]. Small molecule inhibitors, such as vemurafenib, suppress permanently active mutated BRAF that results in the arrest of proliferation and the subsequent death of melanoma cells in vitro and in vivo during patient treatment [1, 7]. A complementary approach to improve the survival of patients with metastatic melanoma is based on the usage of immune-stimulating monoclonal antibodies, which suppress endogenous inhibitors of the immune response: ipilimumab that blocks CTLA-4 [8] and nivolumab that blocks PD-1 receptor [9]. Unfortunately, tumor relapse frequently follows within several months in patients treated with specific molecule inhibitors or after immunostimulation [10, 11].

Resistance of melanoma to therapy is, in general, a result of Darwinian selection among the strongly heterogeneous population of cancer clones with dramatic genomic instability [12], which is accompanied by genetic, epigenetic or microenvironmentally regulated suppression of proapoptotic signaling pathways in these clones in concert with overactivation of the prosurvival and proliferative pathways [13]. Typical examples of the selective pressure for cancer cell survival are overactivation of CRAF after stable inhibition of BRAF [14] and overactivation of STAT3 in the case of use of MEK-ERK inhibitors in melanoma cells [15, 16]. Such compensatory mechanisms for reestablishing activity of critical signaling proteins and enzymes in cancer cells after treatment could be based on metabolic regulation, crosstalk in the cell signaling networks or, finally, on gene mutations. Comprehensive analysis of a landscape of driver mutations in melanoma indeed revealed several novel mutations, including RAC1 P29S (4–9 % of patient's melanomas) that confers resistance to pharmacological inhibition of BRAF [6, 17]. Additionally, a role for activation of Notch1 signaling in promoting resistance to MAPK inhibitors in BRAF V600K mutated cells was highlighted [18]. Hence, a suppression of tumor cell proliferation/survival through combined inhibition of distinctive signaling pathways [19], as well as reestablishing of effective induction of cell death in resistant metastatic melanoma cells appear to be a predominant therapeutic goal. Selection pressure for cancer cell survival may target signal-dependent regulation of gene expression and epigenetic control mechanisms that often precede somatic mutations, which could in turn affect the similar downstream functions. On the other hand, stochastic mutagenesis in dividing cells, especially in conditions favorable to genomic instability, might be the main factor of the creation of somatic clones with numerous mutations, including driver mutations, which predetermine the cell malignancy [20].

However, the original stochastic model of somatic mutagenesis and selection of cancerous clones [12] was challenged by elucidation of cancer initiating cells, which in many cases are close relatives to normal stem cells. The alternative "hierarchical" model suggests that genomic instability at the levels of the self-renewal and differentiation of stem or precursor cells may result in their neoplastic conversion into cancer initiating cells or "cancer stem cells" [21, 22]. According to this model, a tumor at the state of progression is composed of cell subpopulations in different phases of differentiation as a large group of rapidly dividing differentiated cells and a relatively small group of slowly dividing cells with a stem cell-like phenotype. Extensive investigation of cancer initiating cell subpopulations in different types of tumors revealed, however, that the percentage of cancer initiating cells among the total number of cancer cells exhibit a dramatic variation from 0.1 % to almost 100 % [22, 23].

The existence of melanoma initiating cells or "melanoma stem cells" has also been suggested for this type of cancer [24, 25]. However, it still remains a controversial problem [26, 27] due to a strong variation in the percentage of cancer initiating cells in different melanoma lines and patient's samples, in addition to uncertainty in the specificity of biomarkers. Melanoma initiating cells could be identified via expression of different biomarkers such as CD133, ABCB5, NGFR, SOX10, CD20, CD166, and some others [28–32]. However, there is no final consensus on this subject. Therefore, further elucidation of molecular mechanisms underlying the regulation of melanocyte stem cells (melanoblasts) and their possible linkage with the melanoma initiating cells are especially important for the development of novel therapeutic strategies for melanocyte malignancy.

Cancer progression and development, including melanoma, are tightly linked with the regulation of cell death.

Programmed death of normal and cancer cells is executed via two main mechanisms, apoptosis and programmed necrosis (or necroptosis), which are modulated by numerous genetic, epigenetic and metabolic regulators (including misfolded protein stress, macroautophagy and mitophagy) that finally result in positive or negative effects on survival of normal and cancer cells. The significance of the induction of apoptosis (in its two forms, the exogenous death ligand/death receptor-dependent and the endogenous mitochondria-dependent death signaling pathways) to cure cancer is well established [6, 13, 33, 34], while a role for regulated necrosis [35, 36] in cancer cells is still unknown since it is not completely investigated. In the present study, we used several human melanoma cell lines from the subsequent phases of melanoma development (radial growth phase, vertical growth phase and metastatic phase) [37], to compare: (i) frequency and efficiency of the induction of cell death via apoptosis and necroptosis; (ii) the presence of neural and cancer stem cell biomarkers as well as death receptors, DR5 FAS and TNFR1, in adherent and spheroid cultures of melanoma cells; and iii) the ability of melanoma cells to perform neural trans-differentiation.

Results

Expression of regulators of pluripotency and neural stem cell biomarkers in human melanoma lines from the subsequent phases of cancer development

In the present study, we used eight well-characterized melanoma cell lines (Fig. 1a) that were isolated from different phases of melanoma progression [38, 39] with established BRAF and PTEN status [16, 40]; see also a table of melanoma lines with BRAF and PTEN status by M. Herlyn (http://www.wistar.org/lab/meenhard-herlyn-dvm-dsc/page/melanoma-cell-lines-0). Embryonic neural stem cells (NSC), which are in close relation to neural crest stem cells (NCSC), the ancestors of melanoblasts, have been used as reference cells with high levels of expression of master regulators of pluripotency, such as SOX2 and NANOG, and stem cell biomarkers, CD133 and NGFR (Fig. 1b, c). Most of NSC are positive for FAS and TRAIL-R2/DR5 (Fig. 1b) that could be involved in the initiation of death signaling cascades and, alternatively, under specific circumstances in protective signaling in cancer stem cells [41]. NSC are commercially available and could be easily cultured in serum-free media supplemented with EGF (20 ng/ml), FGF2 (20 ng/ml) and insulin (5 μg/ml). Melanoblasts are known as potentially multipotent cells that could differentiate not only into melanocytes but occasionally into neurons and glial cells [42]. U87MG glioblastoma was used as an additional reference cancer cell line with well-established characteristics of gene expression and malignancy. All eight melanoma lines exhibited high protein expression levels of SOX2, with preferential nuclear and perinuclear localization (Fig. 1c). However, Nestin, an early neuroprogenitor marker, was almost completely absent in WM35 radial growth phase (RGP) melanoma cells and was present approximately in 40 % of WM793 vertical growth phase (VGP) melanoma cells (Fig. 1c, d). 1205Lu cells, which were established using a lung metastasis developed in nude mice with human WM793 xenotransplant [43], demonstrated 100 % presence of Nestin. Furthermore, all metastatic melanoma lines used in the current study exhibited high Nestin expression. However, Nestin was not detected in U87MG glioblastoma cells that were positive for SOX2 protein expression (Fig. 1c).

Next we performed a broader comparison of WM35, WM793 and WM9 human melanoma cells, which represented RGP, VGP and metastatic phases, respectively, for the presence of pluripotency markers and critical signaling proteins (Figs. 1 and 2). NSC was again used as reference line. High levels of SOX2 and pronounced levels of NANOG protein expression were detected in these cell lines (Fig. 2a, d). Variable levels of other important transcription factors, such as NF-κB (total and active phosphorylated forms) and STAT3, as well of signaling kinases MAPK p38, ERK1/2 and AKT (total and active forms) were revealed by Western blot assay (Fig. 2d). High levels of phospho-ERK were detected in confocal images of WM9 cells, while the heterogeneous distribution of phospho-ERK among WM793 cells with low, intermediate and high kinase levels was observed. WM35 cells demonstrated low to average levels of basal phospho-ERK and very low, almost undetectable levels of Nestin (Fig. 2a, b). After total protein isolation, decreased basal levels of phospho-ERK (normalized to total ERK and total protein level) were observed in WM35 cells lines using Western blot assay (Fig. 2d). Constitutive activity of ERK in melanoma cells is regulated at two levels (i) via permanently active mutated BRAF and (ii) via inducible activation of growth receptor tyrosine kinases resulting in high levels of CRAF and ERK activity in metastatic melanoma cells [44]. This results in different levels of ERK activity in three melanoma lines, WM35, WM793 and WM9, which have BRAF V600E.

NGFR, a lineage marker of neural crest stem/progenitor cells and melanoma initiated cells [28], was expressed on the surface of a vast majority of WM793 (VGP) and metastatic WM9 cells, but was revealed only at low levels in WM35 (RGF) cells and NSC (Fig. 2c). In contrast, CD133, a potential marker for several types of cancer stem cells, was present at high surface levels in a majority of NSC, modestly on the WM35 surface and as a minor subpopulation (only 1 %) with low surface levels in

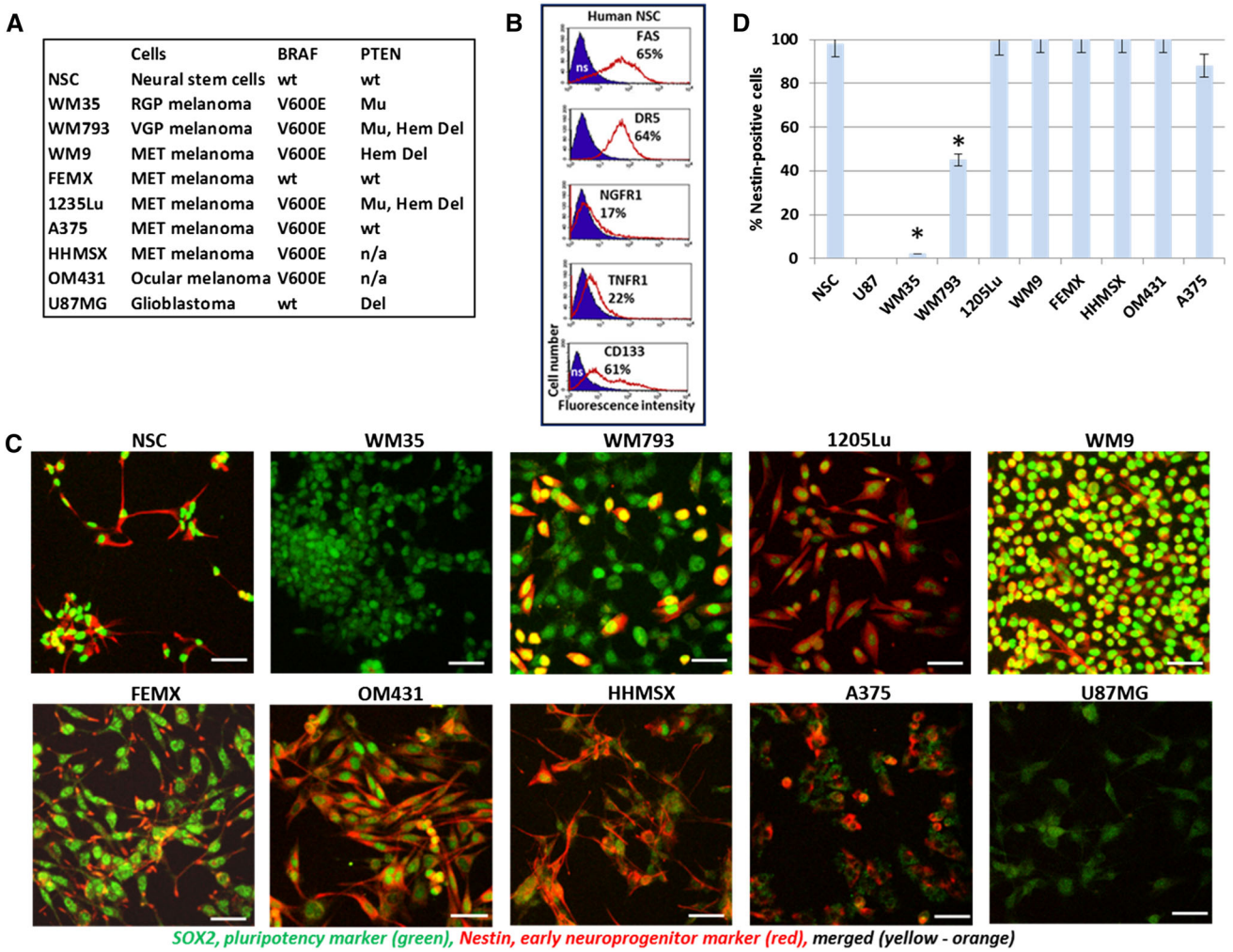

Fig. 1 Human neural stem cells (NSC) and human melanoma cell lines used in this study. **a** NSC, eight human melanoma cell lines and glioblastoma U87MG were used. BRAF status is indicated: BRAF wild-type (wt) protein in human NSC, FEMX metastatic (MET) melanoma and U87MG glioblastoma; BRAF V600E mutated variant in WM35 radial growth phase (RGP) melanoma cells, WM793 vertical growth phase (VGP), WM9, 1235Lu, HHMSX and A375 metastatic (MET) melanoma cells and OM431 ocular melanomas. PTEN status: Wild type (wt), Deleted (Del), Hemi-deleted (Hem Del), Mutated (Mu). **b** Immunostaining and surface expression of indicated receptor in NSC that was determined by FACS analysis; percentage of positive cells is indicated, ns means non-specific staining. **c** Confocal analysis of images after immunostaining using rabbit polyclonal Ab to SOX2, a pluriopotency marker (*green*) and monoclonal antibody to Nestin, an early neuroprogenitor marker (*red*). Bar = 50 μm. **d** Percentage of Nestin-positive cells among melanoma and glioblastoma lines. *Error bars* represent mean ± SD ($p < 0.05$, Student's *t* test). *Stars* indicate significant difference

WM793 and WM9 cells (Fig. 2c). Similarly, TNFR1 and TNFR2 demonstrated intermediate levels of surface expression in NSC, while these receptors were poorly detectable on the surface of melanoma lines (Fig. 2c). After cell permeabilization with 0.5 % NP40, however, high intracellular levels of TNFR1 and other receptors, including CD133 and NGFR, were revealed in WM35 and WM9 cells (see Fig. 3a, b). Both TNFR1 (TNFRS1A) and NGFR (TNFRSF16), members of the Tumor necrosis factor receptor superfamily, possess a similar (initiation of cell death signaling) and numerous specific features linked to signal-dependent regulation of gene expression [45].

We used the exogenous recombinant TNFα (20 ng/ml) alone or in combination with cycloheximide (CHX, 1 μg/ml) for death induction in WM35 and WM9 melanoma cells. TNF-mediated apoptosis was previously observed at prominent levels in human NSC [46]. Pronounced levels of apoptosis in melanoma cells were detected only after combined treatment, suggesting increased availability of TNFR1 for the exogenous TNFα in the presence of CHX. Pan-caspase inhibitor zVAD-fmk (40 μM) partially suppressed TNF and CHX induced apoptosis and levels of total death (Fig. 2e, f). In contrast, the presence of Necrostatin-1 (40 μM), which inhibited RIP1 kinase activity and

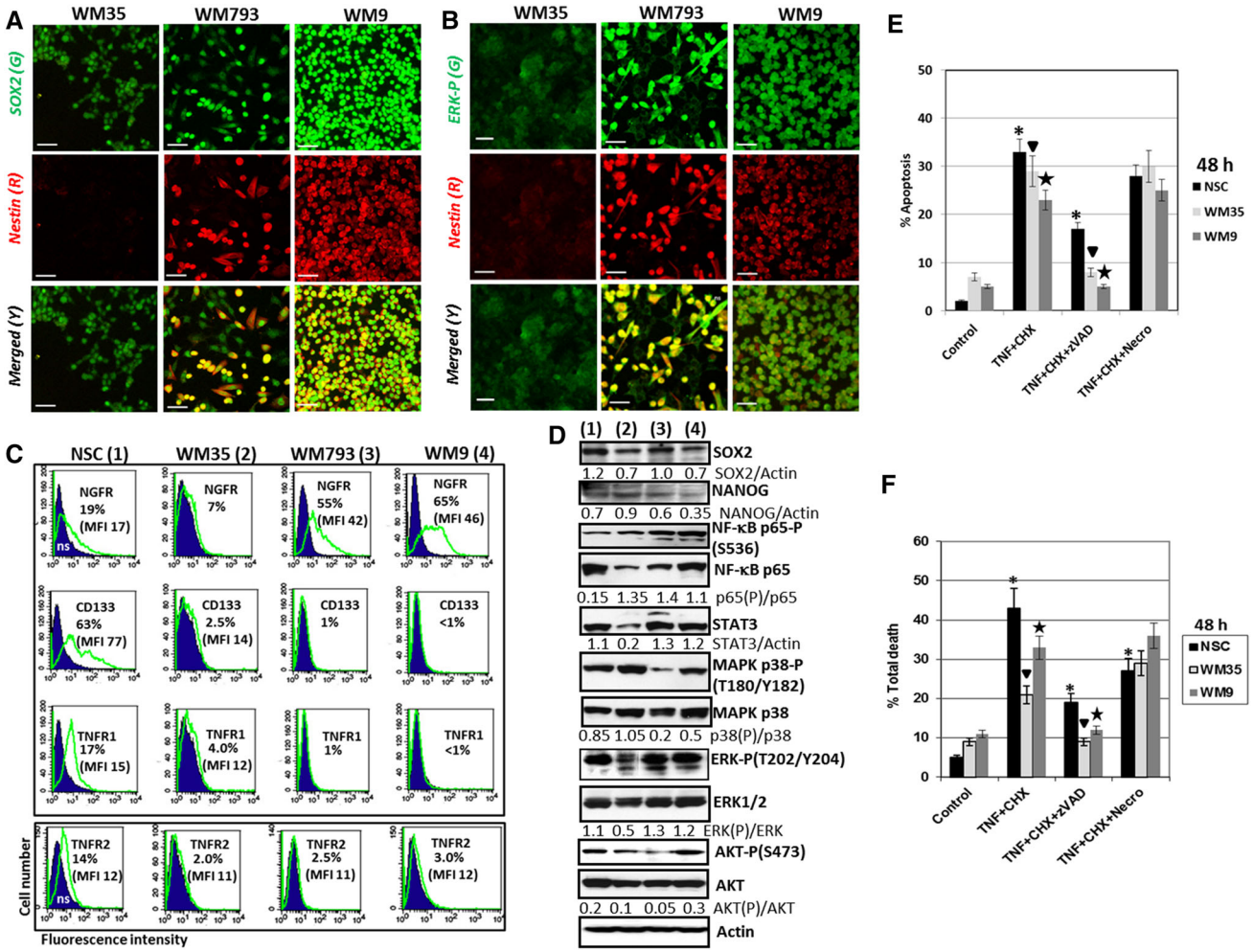

Fig. 2 TNFα/TNFR-mediated cell death in NSC and in human melanoma lines WM35, WM793 and WM9 expressing the neural stem cell markers and TNFR1/2. **a** and **b** Confocal analysis of images after immunostaining using rabbit polyclonal Ab to phospho-ERK (*green*) and monoclonal Ab to Nestin (*red*) or polyclonal Ab to SOX2 (*green*) and monoclonal Ab to Nestin (*red*); merged images in yellow/orange. *Bar* = 50 μm **c** Surface expression levels of NGFR, CD133 and TNFR1/2 in NSC and melanoma lines; *ns* nonstained cells. Percentage of antigen-positive cells is indicated. **d** Western blot analysis of protein expression levels of SOX2 and NANOG, pluripotency markers, as well as signaling proteins and transcription factors in NSC (1) and specified melanoma lines (2–4). **e** Cell cycle-apoptosis analysis of WM35 and WM9 melanoma cells after treatment with cycloheximide (CHX) 1 μM, TNFα (20 ng/ml), zVAD (40 μM) alone or in combination. 48 h after treatment, cells were stained with PI and analyzed by the flow cytometry. **f** Total death levels were determined by Trypan blue exclusion assay. Pooled results of four independent experiments with indicated treatments are shown for NSC, WM35 and WM9 cells. zVAD, 40 μM and Necrostatin (Necro), 40 μM were used. *Error bars* represent mean ± SD ($p < 0.05$, Student's *t* test). *Stars* and *triangulars* indicate significant differences

programed necrosis, partially decreased levels of total cell death in NSC, but not in WM35 and WM9 melanoma cells. It indicated a parallel development of necroptosis and apoptosis in NSC and the apparent absence of necroptotic commitment in WM35 and WM9 cell after TNF+CHX treatment (Fig. 2f). Interestingly, a permeabilization of WM35 and WM9 melanoma cells (which were cultured in complete media containing 10 % FBS) with 0.5 % NP40 followed by immunostaining and FACS analysis demonstrated high intracellular pools of NGFR, TNFR1 and CD133 in two melanoma lines, while the vast majority of DR5 (TRAIL-R2) was already located on the cell surface (Fig. 3a, B and not shown). This was correlated with high sensitivity of these melanoma lines to TRAIL-induced apoptosis.

WM35 cells, similar to NSC, formed spheroids in serum-free media supplemented with FGF2 (20 ng/ml), EGF (20 ng/ml) and insulin (5 μg/ml) (Fig. 3c, d), and were able to further grow as a spheroid culture. In contrast, WM9 metastatic melanoma formed two subpopulations of floating (live and dead) and adhering (live) cells in serum-free media, but most of the cells finally died after 8 days in these conditions (Fig. 3d). Additionally, WM35 spheroids demonstrated decreased surface expression of DR5 and acquired resistance to TRAIL-mediated apoptosis,

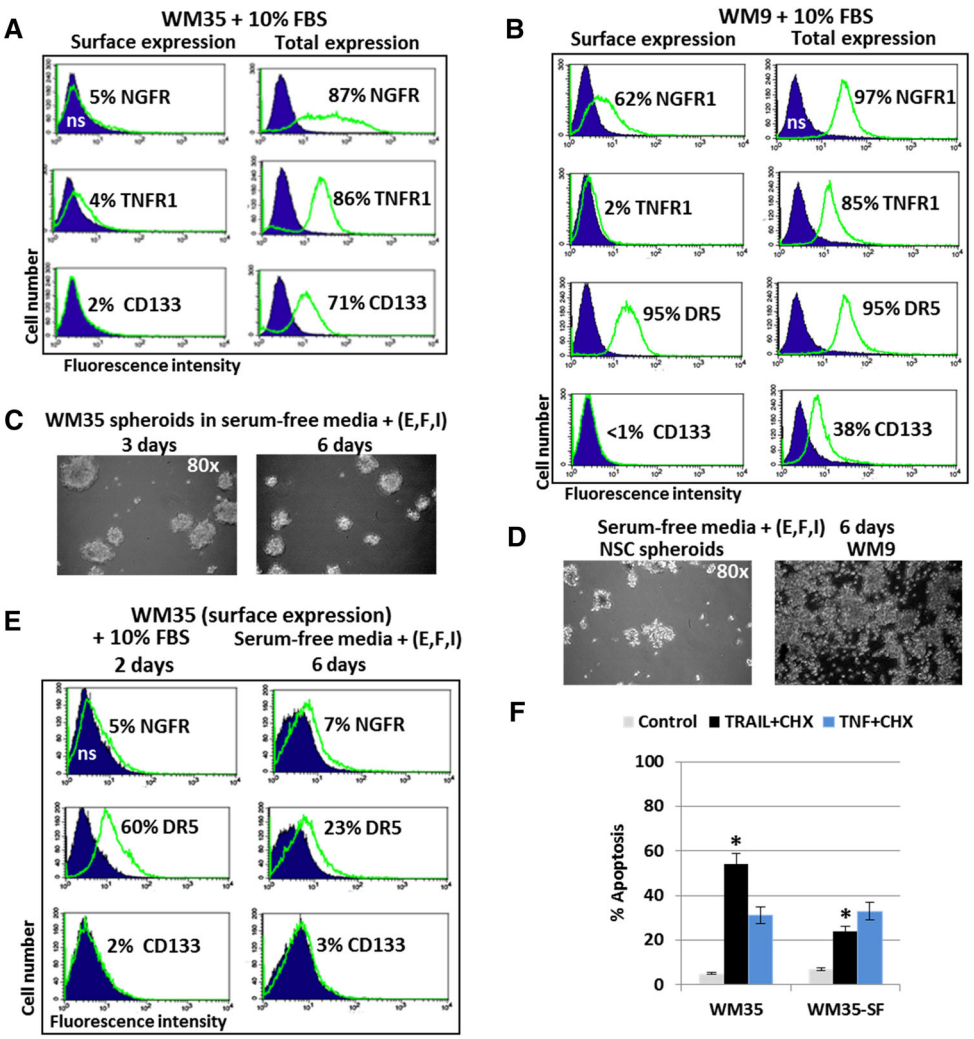

Fig. 3 Receptor expression and spheroids formation in WM35 and WM9 melanoma cell lines. **a** and **b** Surface and total expression levels of NGFR, TNFR1, FAS and CD133 in WM35 and WM9 human melanoma lines. % Antigen-positive cells are indicated. **c** Spheroid formation by WM35 cells in serum-free media supplemented with FGF2 (20 ng/ml), EGF (20 ng/ml) and insulin (5 μg/ml). Phase-contrast images are shown. **d** NSC (control) and WM9 melanoma cells after 6 days of incubation in the similar serum-free media with supplements. **e** Surface expression of indicated receptors on WM35 cells after cell culture growth in two types of media. **f** Apoptotic levels after treatment of WM35 cells that were grown on the complete (WM35) or serum-free media with supplements (WM35-SF). Apoptosis was induced by combination of TRAL (50 ng/ml) + CHX (1 μg/ml) or TNFα (20 ng/ml) + CHX. Levels of apoptosis were determined using PI staining and cell cycle-apoptotic analysis. *Error bars* represent mean ± SD ($p < 0.05$, Student's *t* test). *Stars* indicate significant difference

compared to cells that were cultured in the complete media (Fig. 3e, f). In contrast, low surface, but high total expression of TNFR1 in WM35 spheroids maintained relatively stable levels of TNF-mediated apoptosis (Fig. 3f). We hypothesized that the WM35 early melanoma cell population was enriched by potential cancer initiating cells, which became more evident in stress conditions, such as apoptotic commitment or growth as a spheroid culture in serum-free media. Indeed, previously published data demonstrated increased tumorigenicity of WM35 cells from spheroid culture, compared to the WM35 adherent culture [47].

The integrity of mitochondria in the cell and general cell survival are strongly dependent from two signaling pathways PI3K-AKT and IKK-NF-κB [48, 49]. Furthermore, IKK-NF-κB pathway controls expression of numerous genes, including genes encoding proinflammatory cytokines, *TNFSF1A (TNFα)*, *IL6* and *IL8*, and *COX2* [48, 50]. Since PTEN, an endogenous inhibitor of PI3K-AKT pathway, is frequently mutated/deleted in melanomas [3], the basal AKT activity could be well pronounced in melanoma lines. To elucidate the possibility of the induction of mitochondrial death pathways in NSC and WM35 or WM9 melanoma cells, we used a strong proapoptotic potential of combined inhibition of these main survival pathways by small molecule inhibitors of IKKβ-NF-κB (BMS345541) and PI3K-AKT (LY294002) (Suppl. Figure 1). We recently observed high levels of apoptosis induced by such treatment in glioblastoma cells [51]. A combination of BMS345541 and LY294002 (40 μM) induced pronounced levels of apoptotic and total death in NCS 48 h after treatment. As expected, zVAD-fmk, a pan-caspase inhibitor (40 μM), suppressed apoptotic death and increased NSC survival. In contrast, necrostatin cotreatment did not affect cell death levels (Suppl. Figure 1a, b). Interestingly, combined treatment by inhibitors had a dramatic effect on the induction of apoptosis in metastatic WM9 cells, but only modest effects in the primary WM35

cells (that were even less pronounced than effects in NSC) (Suppl. Figure 1c–e). A substantial difference between RGF WM35 and metastatic WM9 melanoma cells in the response to IKK-NF-κB inhibition appears to reflect a distinctive role for inflammatory gene expression [52] during melanoma progression. Caspase inhibitor zVAD-fmk (rather than Necrostatin-1) substantially down-regulated levels of total and apoptotic death in WM9 cells (Suppl. Figure 1c–e). SB203580, a MAPK p38 inhibitor, did not change the proapoptotic effects of BMS345541 in both WM35 and WM9 cells (Suppl. Figure 1d). Taken together, the data obtained demonstrate a prevalence of apoptotic versus necroptotic response in WM9 melanoma cells after treatment with the indicated inhibitors. In contrast, WM35 cells exhibited pronounced resistance to apoptotic and necrotic death in these conditions.

WM793 and FEMX melanoma cells with low metastatic potential: regulation of cell death and stemness

We additionally performed a comparison of WM793 (VGP; BRAF V600E) and FEMX (low metastatic; BRAF wt) melanoma cells, which have previously demonstrated functional and metabolic similarity [53]. Both WM793 and FEMX cell lines exhibited high levels of SOX2 expression with a preferential nuclear localization, and already mentioned a substantial difference in levels of Nestin expression and its location (Figs. 1c and 4a). We hypothesized that the WM793 cell population consisted of two subpopulations of the "early" (Nestin-negative) and "more mature" (Nestin-positive) cells. High levels of phospho-ERK are colocalized with Nestin-positive WM793 cells (Fig. 4a). In contrast, all FEMX cells were Nestin-positive with relatively low Nestin levels in the cell bodies and with pronounced localization of Nestin in the cell neurites. Furthermore, CD133 and COX2 protein expression was almost undetectable in WM793 cells, while it was easily detected in the FEMX cells (Fig. 4a). The difference in total CD133 expression levels between two melanoma lines was really striking. FACS analysis also revealed a difference in surface receptor expression in WM793 versus FEMX cells (Fig. 4b). Indeed, surface expression levels of CD133 could be detected in 9 % FEMX and 2 % WM793 cells. Total levels of CD133 (after cell permeabilization) were substantially higher in FEMX cells compared to WM793: 19 % positive cells with 29 MFI and 3 % positive cells with 15 MFI, respectively (Fig. 4b, c). On the other hand, EGFR and NGFR surface expression was significantly downregulated in FEMX, compared to WM793 cells (Fig. 4b). It should be mentioned that the FEMX cell population represented a combination of multiple clones, and prolonged selection allowed to isolate both low metastatic and high metastatic subpopulations [54].

We addressed probable differences in the induction of distinct cell death pathways in WM793 and FEMX melanoma lines. First, we investigated regulation of cell signaling pathways in WM793 and FEMX cells by small molecule inhibitors, BMS345541 and LY294002 (40 μM), 4-8 h after treatment (Fig. 5a, b). Certain differences in SOX2 protein levels, but relatively similar levels of NANOG were observed in WM793 compared to FEMX cells before and after the indicated treatment. Combined treatment by BMS345541 and LY294002 increased protein expression of SOX2 in both melanoma lines. Second, there was an asymmetry in action of these inhibitors: LY204002 alone and, especially, in combination with BMS345541 decreased levels of phospho-AKT in WM793 cells, but not in FEMX cells 4 h after treatment. On the other hand, both BMS345541 and LY204002 alone or in combination efficiently decreased the ratio of phospho-IKK/total IKK, while the ratio of phospho-p65/total p65 NF-κB did not reflected changes in IKK activity (Fig. 5a). On the other hand, ERK1/2 activity increased upon suppression of AKT and IKK in WM793 cells. Treatment with BMS345541 alone strongly increased p53 protein levels (Fig. 5a). Activation of Capase-9 and Caspase-3 via specific cleaved forms and Capase-3-dependent inactivation of PARP-1 by its cleavage were modestly induced after treatment with LY204002 alone and dramatically increased after combined treatment with LY204002 and BMS345541 in WM793, but not in FEMX cells (Fig. 5a). A similar picture of PARP-1 cleavage was also observed 8 h after combined treatment (Fig. 5b). In contrast, high protein expression of cFLIP p55 and p32 was observed in FEMX, but not in WM793 cells (Fig. 5a).

To determine the extent of the induction of apoptosis and total cell death in WM793 and FEMX melanoma cells after small molecule inhibitor treatment, we used several approaches: (i) cell cycle-apoptosis analysis of PI stained nuclei 48 h after treatment followed by flow cytometry (Fig. 5b; Suppl. Figure 2b); and (ii) detection of levels of total death using Trypan blue staining and light microscopy (Fig. 5d, e); (iii) the pan-caspase inhibitor zVAD (40 μM) was used to further confirm the involvement of caspase-dependent apoptotic signaling pathways. Results of cell cycle-apoptosis analysis (48 h after treatment) clearly demonstrated the protective effects of zVAD, but not Necrostatin-1 (both at dose 40 μM) on apoptotic death induced by a combination of BMS345541 and LY294002 (Fig. 5b; Suppl. Figure 2b). Non-efficient suppression of AKT activity by LY204002 alone or in combination with BMS345541 in FEMX cells correlated with their resistance to proapoptotic treatment (Fig. 5b). Finally and surprisingly, total levels of cell death induced by BMS345541 and LY294002 alone or in combination were significantly

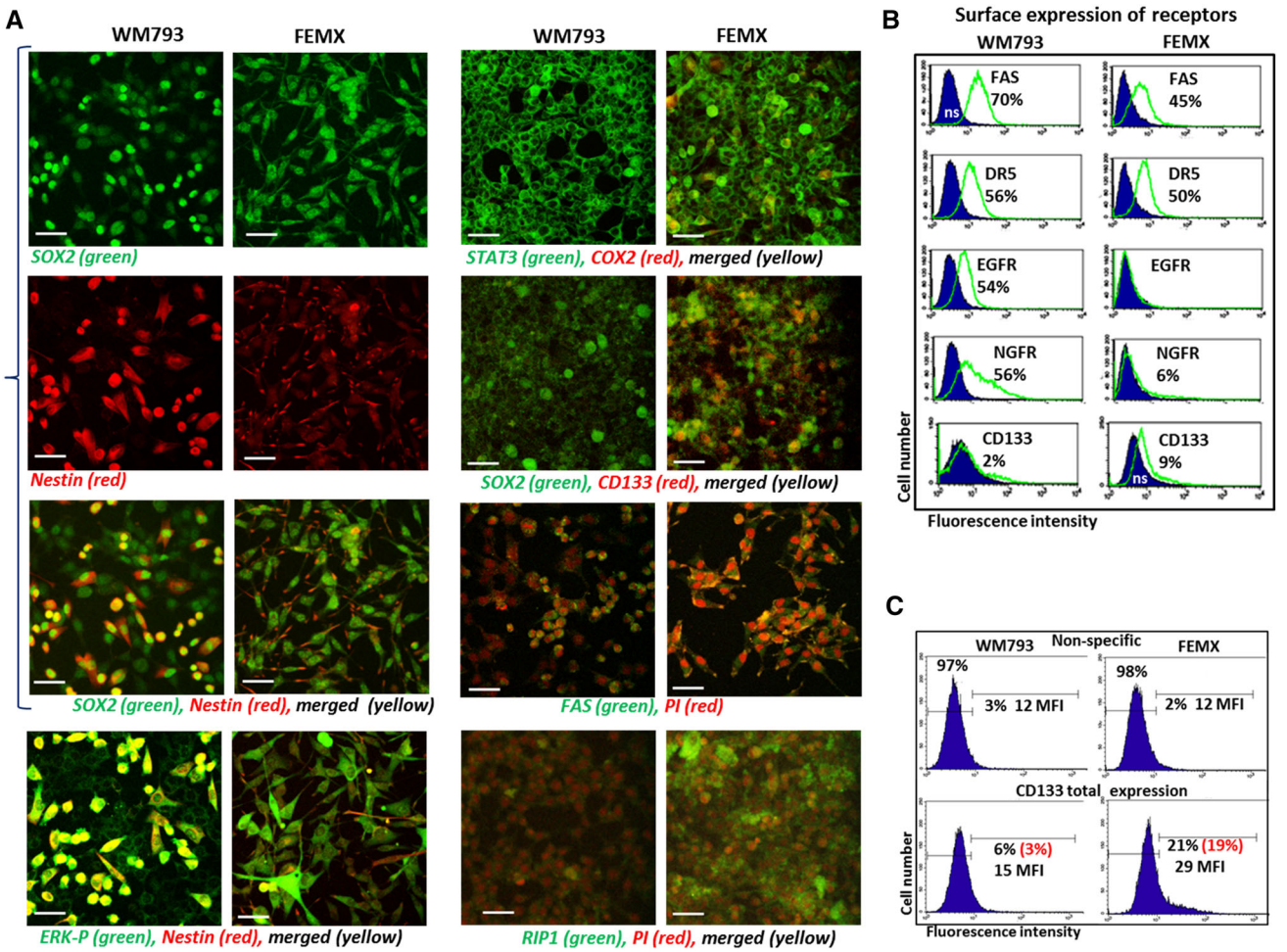

Fig. 4 Melanoma cell lines, WM793 and FEMX, express stem cell and proapoptotic markers. **a** Confocal analysis of images after immunostaining using rabbit polyclonal Ab to SOX2, a pluriopotency marker (*green*) and monoclonal antibody to Nestin, an early neuroprogenitor marker (*red*). *Bar* = 50 μm. An additional immunostaining with anti phospho-ERK (*green*) and anti-Nestin (*red*), anti-STAT3 (*green*) and anti-COX2 (*red*), anti-SOX2 and anti-CD133, anti-FAS (*green*), anti-RIP1 (*green*) Abs was also performed. **b** Surface expression levels of NGFR, CD133, FAS, DR5 and TNFR1 in NSC and WM793 and FEMX melanoma cells. Percentage of positive cells is indicated. **c** CD133 total expression in WM793 and FEMX cells was determined after permeabilization of the plasma membranes with 0.5 % NP40 and immunostaining followed by FACS analysis. Median fluorescence intensity (MFI) and % positive cells (in *red*, after subtraction of nonspecific level) are shown

decreased in FEMX but not in WM793 cells by Necrostatin-1 (Fig. 5c). This indicates involvement of necroptosis in the induction of death of FEMX cells. Levels of RIP1, a critical signaling kinase for induced necroptosis, were substantially higher in FEMX cells compared to WM793 cells based on immunostaining and confocal microscopy (Fig. 4a, the bottom panel) or Western analysis (Fig. 5a).

Since Western blotting also demonstrated an upregulation of MAPK p38 levels by BMS345541 (Suppl. Figure 2a), we additionally used a combination of BMS345541 and SB203580 (an inhibitor of p38) for upregulation of apoptosis in melanoma cells. Combined treatment with these inhibitors further increased apoptotic levels in WM793, indicating a prosurvival role for both IKKβ and MAPK p38 (Suppl. Figure 2b). As expected, the presence of zVAD decreased apoptotic levels induced by these inhibitors. In general, combined treatment with BMS345541 and LY294002 demonstrated strong death-inducing effects via apoptosis and/or necroptosis in some melanoma lines, such as WM9 and WM793 and several others, but was not a universal inducer of high levels of cell death for other melanoma cells, such as WM35 or FEMX, probably due to a compensatory activation of alternative pathways.

In contrast, TRAIL in combination with CHX effectively induced TRAIL/DR5-mediated apoptosis and upregulated total death levels in both WM793 and FEMX cells, due to evident surface expression of DR5/TRAIL-R2 (Suppl. Figure 2c, d). Since both WM793 and FEMX cells produce and secrete IL8 at high levels (Fig. 2e), we added

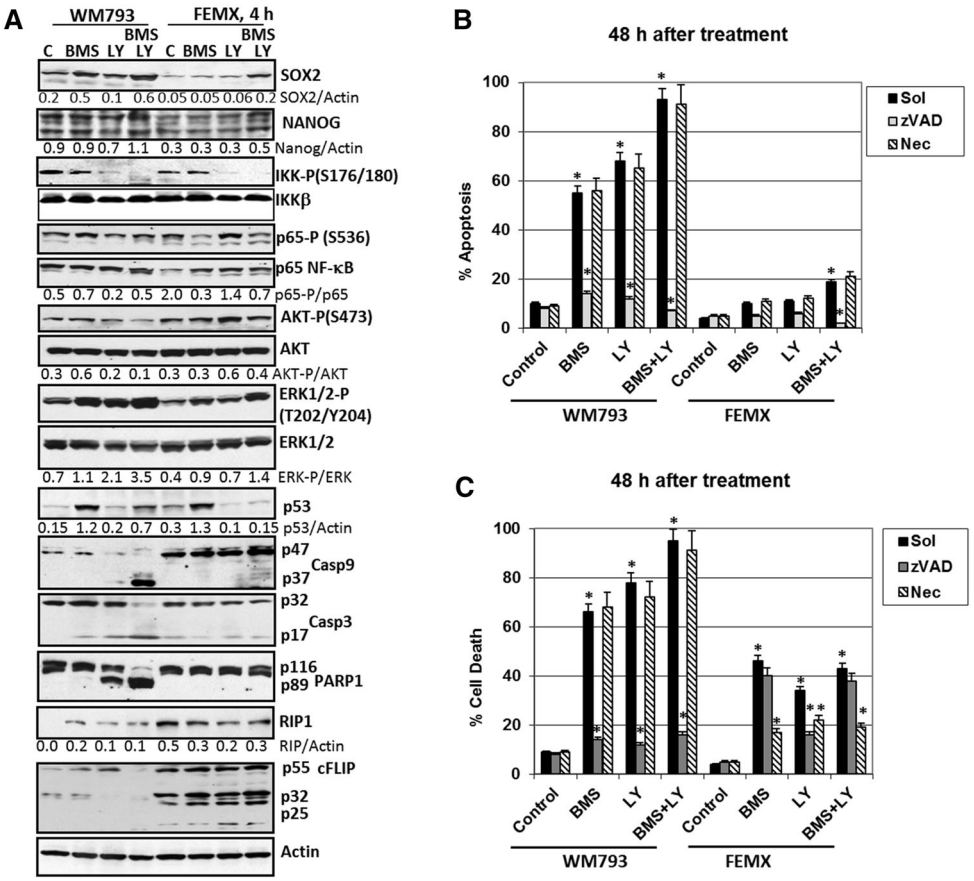

Fig. 5 Effects of small molecule inhibitors BMS345541 and LY294002 on cell signaling proteins and their downstream targets in WM793 and FEMX melanoma cells. **a** Western blot analysis of indicated proteins was performed 4 h after treatment of cells with BMS345541 (20 μM) and LY294002 (40 μM) alone or in combination. **b** Cell cycle-apoptosis analysis was performed 48 h after BMS345541 and LY294002 treatment using PI staining and FACS analysis. **c** Total cell levels were detected by Trypan blue staining. Pooled results of four independent experiments with the indicated treatments are shown for WM793 and FEMX cells. zVAD (40 μM) and Necrostatin (Nec, 40 μM) were used. *Error bars* represent mean ± SD ($p < 0.05$, Student's *t* test). *Stars* indicate significant difference

anti-IL8 inhibitory antibody (5 μg/ml) before initiation of TRAIL-mediated apoptosis. Apoptotic levels were notably increased in these conditions (Suppl. Figure 2f). This highlights an anti-apoptotic role for endogenous IL8 secretion in melanoma cells. Interestingly, TRAIL+CHX induced relatively similar levels of apoptosis in WM793 and FEMX cells, in spite of increased levels of cFLIP (p55, p32 and p25) in FEMX cells (Fig. 5a). Since FEMX cells possess substantially higher levels of RIP1 (Figs. 4a and 5a), we decided to evaluate induction of necroptosis in FEMX cells using the canonical TNFα+CHX treatment.

We previously observed efficient induction of both apoptosis and necroptosis by TNFα+CHX in NSC, which possess high surface expression of TNFR1/2 (Fig. 2c). However, TNFR surface expression was detected at low levels in most melanoma lines. In contrast, total intracellular levels of TNFR1 in WM793 and FEMX cells were relatively high (Fig. 6a). Both melanoma lines expressed RIP1, with the highest levels in FEMX (Figs. 4a and 5a). Cell cycle-apoptosis analysis demonstrated substantial levels of TNF+CHX induced cell death in WM793 and FEMX melanoma cells, which, however, were not suppressed until the basal levels of cell death in the presence of zVAD in FEMX cells (Fig. 6b, c). On the other hand, Necrostain-1 (40 μM), an inhibitor of RIP1 kinase activity and necroptosis, substantially downregulated levels of total death induced by TNF+CHX combination in FEMX, but not in WM793 cells (Fig. 6d). These data demonstrated a prominent TNF-induced necroptosis in FEMX cells.

We further compared the capacity of WM793 and FEMX cells to form spheroid cultures and to grow in serum-free media supplemented with EGF, FGF2 and insulin (Fig. 7). FEMX cells could effectively form spheroids, while WM793 started to die in these condition 4 days after media transfer (Fig. 7c, d). Interestingly, surface expression of receptors (NGFR, DR5 and CD133) was decreased in serum-free media (Fig. 7a, b) and was correlated with decreased levels of TRAIL-mediated death of FEMX cells 24 h after treatment by TRAIL+CHX, while levels of TNF-mediated apoptosis were not changed (Fig. 7e). An additional ability for survival of FEMX cells in stress conditions was probably correlated well with pronounced endogenous COX2 expression, which is critical for prostaglandin E2 (PGE2) production followed by the autocrine and paracrine activation of PGE2-EP2/4 signaling pathway [55]. NF-κB-dependent COX2 expression could be further upregulated by exogenous TNFα (Fig. 7f).

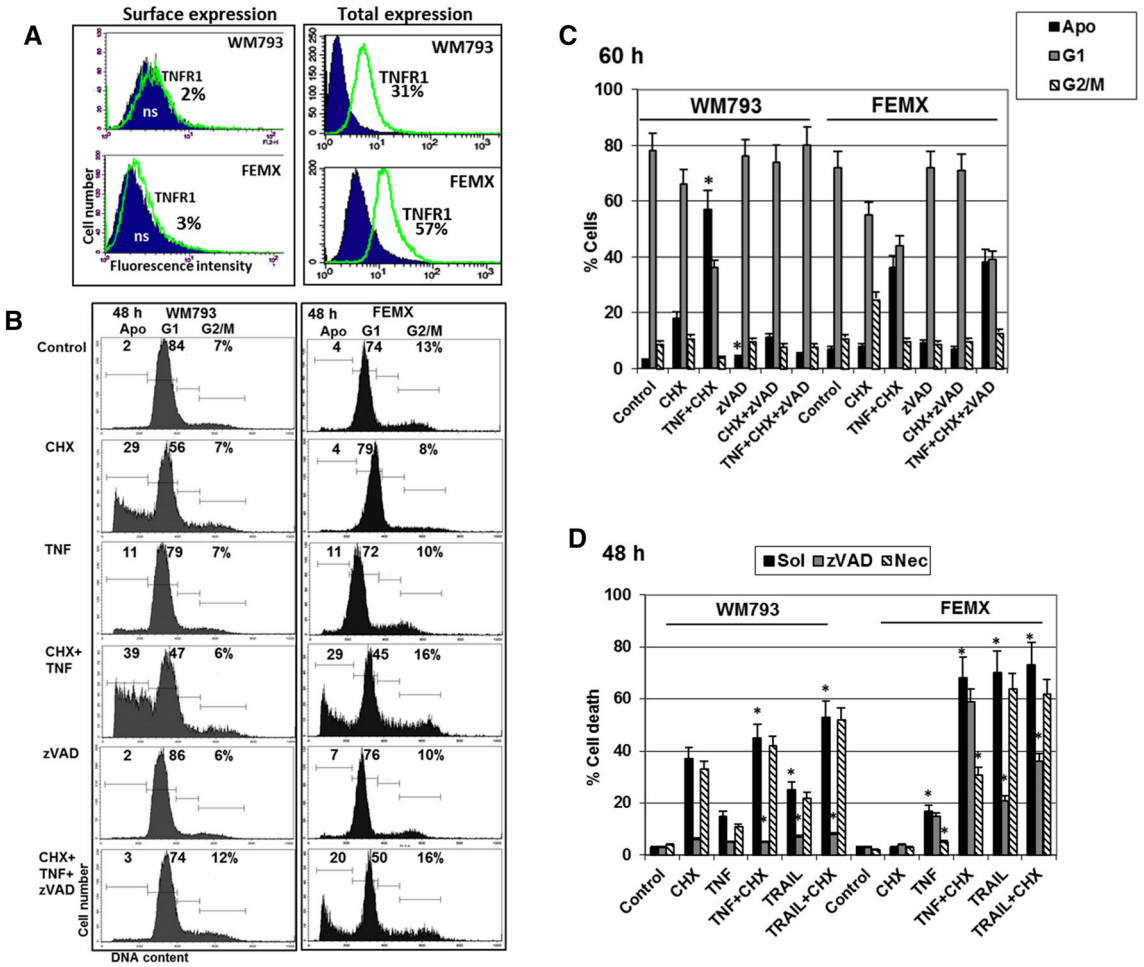

Fig. 6 Total and apoptotic death induced by TNFα and cycloheximide treatment of WM793 and FEMX melanoma cells. **a** Surface and total TNFR1 expression in WM793 and FEMX melanoma cells. Percentage positive cells is indicated; ns, non-specific staining. **b** and **c** Cell cycle-apoptosis analysis of WM793 and FEMX melanoma cells after treatment with cycloheximide (CHX) 1 μM, TNFα (20 ng/ml), zVAD (40 μM) and Necrostatin (40 μM), alone or in combination. 48-60 h after treatment, cells were stained with PI and analyzed by the flow cytometry. Percentage of cells at the cell cycle phases is indicated in panels (**b**) and (**c**). **d** Total death levels were determined by Trypan blue exclusion assay. Pooled results of four independent experiments are shown for WM793 and FEMX melanoma cells. *Error bars* represent mean ± SD ($p < 0.05$, Student's *t* test). *Stars* indicate significant differences between the mock control cells, which were treated in the absence of zVAD or Necrostatin (Sol, 0.1 % DMSO), and cells that were treated with indicated reagents in the presence of zVAD (40 μM) or Necrostatin (40 μM)

COX2 upregulation could increase survival function in many types of cancer cells including melanoma [56, 57].

Metastatic 1205Lu, A375, HHMSX and OM431 melanoma cells: biomarkers, stemness, resistance to apoptosis and ability for trans-differentiation

As mentioned above, the 1205Lu melanoma line was established using a lung metastasis originated from human xenotransplant of WM793 melanoma cells in a nude mouse [43]. Similarity and differences between the primary WM793 cells and metastatic 1205Lu cells in signaling pathways and apoptotic resistance were previously described [53, 58]. One of the new differences discovered in the current study was levels of Nestin protein expression in these melanoma lines: there were two subpopulations (negative and positive for Nestin) in WM793 and quite homogenous distribution of Nestin in the 1205Lu cell population (Figs. 1b and 2a, b). The basal phospho-ERK demonstrated preferentially cytoplasmic location in both lines (Figs. 2b and 8a). As we also demonstrated above, all metastatic melanomas used in the present study, including A375, were Nestin-positive with pronounced levels of Nestin and SOX2 (Figs. 1c, d and 8a). 1205Lu cells expressed substantial levels of NGFR, TNFR1, FAS and DR5 on the cell surface, while the A375 cell line demonstrated surface expressing of NGFR and TNFR1 only among subpopulations of cells (Fig. 8b, c and e). Surface

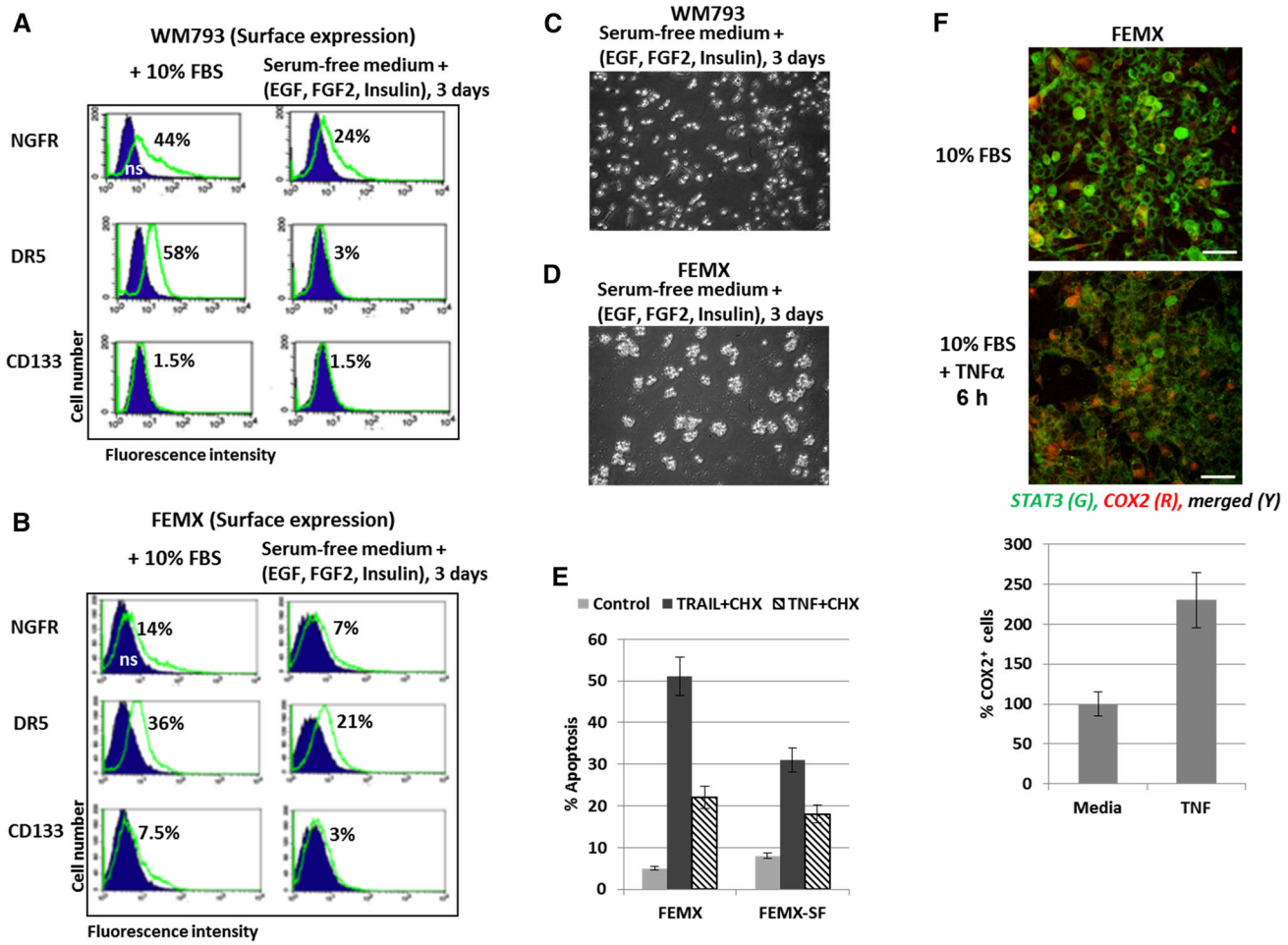

Fig. 7 Surface and total expression of receptors and TRAIL-induced apoptosis in WM793 and FEMX melanoma cells that were grown as adherent (media with 10 % FBS) or suspension (serum-free media with supplements) cell cultures. **a** and **b** Surface expression of receptors in WM793 and FEMX cells after culture in the complete media or growth in serum-free media with supplements: EGF (20 ng/ml, FGF2 (20 ng/ml) and insulin (5 μg/ml). Immunostaining receptors and the flow cytometry were performed. **c** and **d** Spheroid culture of FEMX cells and mixed (adherent and floating) culture of WM793 were observed after culturing in serum-free media with supplements. **e** TRAIL+CHX and TRAIL+TNF-induced apoptosis was induced by 24 h-treatment of FEMX cells grown before treatment in the complete media (for 2 days) or serum-free (SF) media with supplements (for 3 days). PI staining of the cell nuclei and FACS analysis were performed for the detection of apoptotic levels. **f** Effects of TNFα (20 ng/ml) on expression levels of COX2 8 h after treatment of FEMX cells. Confocal images are shown after immunostaining with anti-STAT3 (*green*) and anti-COX2 (*red*) Abs. The bottom panel demonstrates relative increase of COX2-positive cells after TNF treatment

expression of CD133 was quite noticeable in 1205Lu but not seen in A375 cells. Surprisingly, A375 spheroid cultures could grow in serum-free media with supplements, while 1205Lu cells did not produce spheroids in these conditions. Instead, 1205Lu cells survived and could continue differentiation as an adherent culture (see Suppl. Figure 4). Interestingly, the levels of surface expression of several receptor proteins were not really decreased in A375 spheroid culture (Fig. 8e). These receptor proteins were also maintained in 1205Lu cells at relatively equal levels in both the complete media and serum-free media (data not shown). This correlated with the high levels of receptor-mediated cell death (via DR5 or FAS) for both melanoma lines independently of growth media; at the same time, TNF-induced death was substantially higher in 1205Lu cells (Fig. 8g) due to efficient surface expression of TNFR1 (Fig. 8b) and was executed via the apoptotic pathway.

Two additional metastatic lines, OM431 ocular melanoma and HHMSX melanoma also expressed SOX2 and Nestin in concert with phospho-ERK and STAT3 (Suppl. Figure 3A). One third of the OM431 cell population was positive for surface NGFR, which was present, however, at high levels inside the cells. The modest level of surface expression was characteristic for FAS, while TNFR1, DR5 and CD133 were barely detectable on the cell surface, even though they were present inside OM431 cells at high or intermediate levels (Suppl. Figure 3B and C). On the other hand, HHMSX cells had very low levels of surface

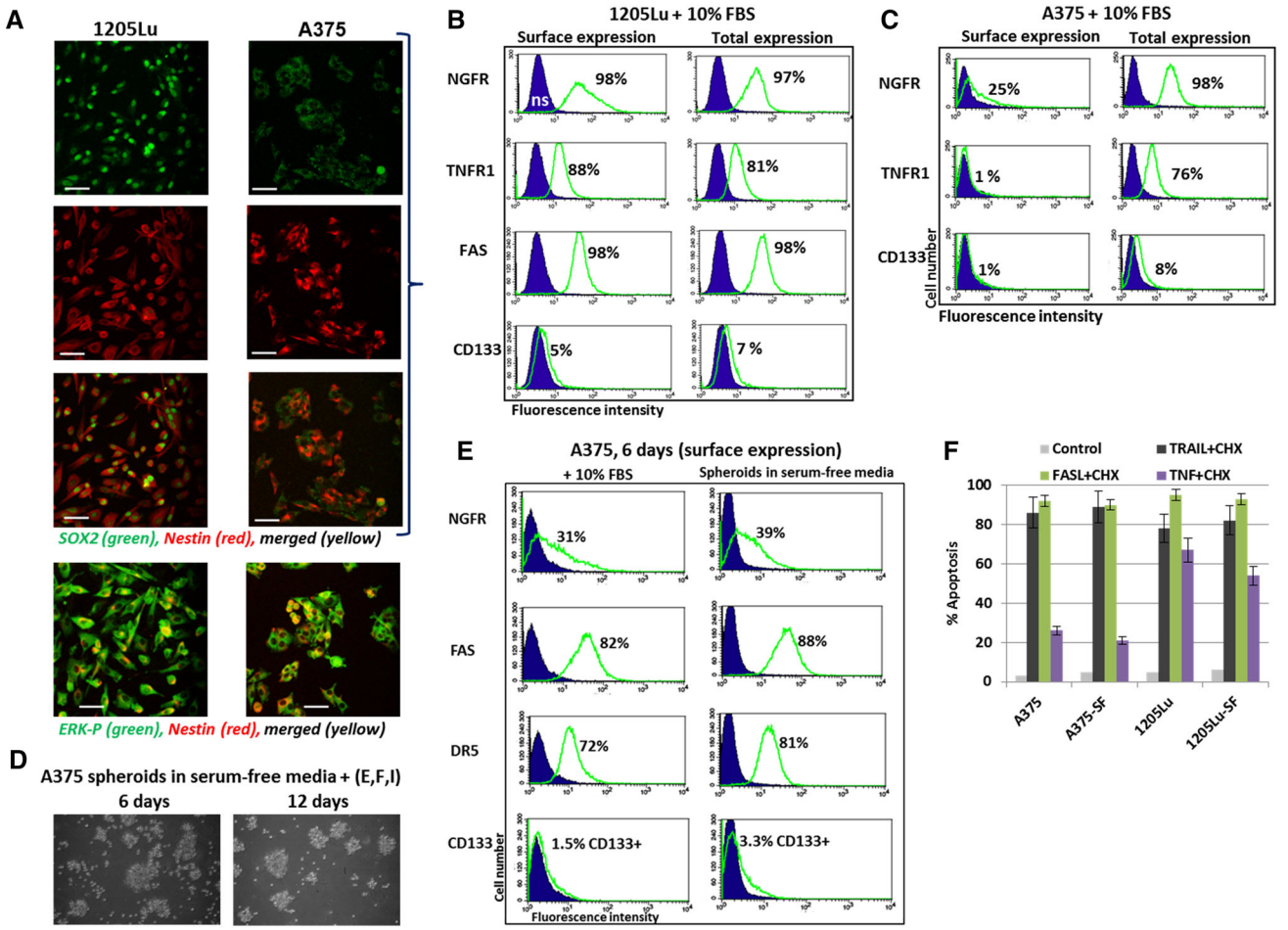

Fig. 8 Metastatic melanoma lines, 1205Lu and A375, express stem cell and proapoptotic markers. **a** Confocal analysis of 1205Lu and A375 metastatic cells after immunostaining using rabbit polyclonal Ab to SOX2, a pluriopotency marker (*green*) and monoclonal antibody to Nestin, an early neuroprogenitor marker (*red*). *Bar* = 50 μm. An additional immunostaining with anti-ERK-P and anti-Nestin Abs was also performed. **b** and **c** Surface and total expression levels of NGFR, TNFR1, CD133, FAS and DR5 in A375 and 1205Lu melanoma cells. Percentage of positive cells is indicated. Total expression levels in 1205Lu and A375 cells were determined after permeabilization of the plasma membranes with 0.5 % NP40 and immunostaining followed by FACS analysis**. d** and **e** A375 spheroids in serum-free media with supplements: EGF, FGF2 and insulin. Surface expression of receptors in A375 spheroids is shown on panel (**e**). **f** Comparison of apoptotic levels in A375 cell and 1205Lu cells after culturing in the complete or serum-free (SF) media with supplements

expression of NGFR, TNFR1 and CD133, although these proteins could be detected inside the cells (Suppl. Figure 3B).

Both OM431 and HHMSX cells could grow in serum-free media with supplements, and produced irregular spheroids (Suppl. Figure 3A, the bottom panel); OM431 spheroids contained decreased levels of surface receptor proteins (Suppl. Figure 3C). The native OM431 and HHMSX cells only slightly responded to FasL- or TRAIL-induced apoptotic signaling. However, TNF+CHX could induce low to average levels of total cell death in HHMSX and OM431 and this could be partially suppressed by either zVAD or Necrostatin-1. This demonstrated a mixed type of cell death signaling that resulted in both apoptosis and necroptosis in OM431 cells (Suppl. Figure 3D). Taken together, our data demonstrated that well pronounced necroptosis was induced by a combination of TNF and CHX in parallel with apoptosis in NSC as well as in FEMX and OM431 melanoma cells. All three lines expressed high levels of RIP1 (Fig. 5a and data not shown) and total TNFR1, which was detected on the cell surface of NSC, but mostly inside FEMX and OM431 cells.

Growth and differentiation of melanoma cell lines in serum-free media with supplements

Suppl. Figure 4 demonstrates a summary picture of the ability of melanoma cells to grow as spheroid cultures in serum-free media supplemented with EGF (20 ng/ml), FGF2 (20 ng/ml) and insulin (5 μg/ml). Interestingly,

classic spheroid structure was characteristic of WM35 melanoma cells. Low-metastatic FEMX cells could also grow as spheroids composed of relatively small numbers of cells. WM793 and WM9 cells died several days after transfer to serum-free media. OM431, A375 and HHMSX cells produced irregular spheroid cultures also containing cell suspension. Finally, 1205Lu adherent cells continued a process of differentiation. HHMSX spheroid structures were attached to dish's matrix in serum-free media. Hence, the ability to grow as a spheroid culture was a characteristic feature for several melanoma lines used. Most of melanoma lines did not notably increase the percentage of CD133-positive cells after culturing as spheroids with but one exception: HHMSX spheroids in serum-free media supplemented with insulin (independently of the presence of the exogenous EGF and FGF2) demonstrated an increase in the levels of CD133-positive cells (Suppl. Figure 5d, e). Increasing expression of CD133 in HHMSX cells is reminiscent of the upregulation of CD133 expression in spheroids of U97MG glioblastoma [51, 59].

Transfer to more restricted conditions, the serum-free media supplemented only by insulin (5 μg/ml) without EGF and FGF2, accelerated the trans-differentiation process for 1205Lu and OM431 cells along the neuronal pathway. Indeed, well pronounced growth of neurites that contained both Nestin, a neuroprogenitor marker, and doublecortin, a neuronal marker, was detected in 1235Lu and OM431 metastatic melanoma cells (Fig. 9). The presence of an additional neuron-specific marker, beta-3-tubulin, was also observed (Suppl. Figure 5a). These events occurred in concert with nuclear translocation of phospho-ERK and STAT3 (Fig. 9, Suppl. Figure 5a). Even at substantially low levels, compared to young neurons, growth of neurites in 1205Lu and OM431 cells was significant in the neuronal differentiation media (Fig. 9e, f; Suppl. Figure 5a). A role of Rac1 in neuronal growth by regulating the cytoskeleton of the growth cone has been well established [60, 61]. Furthermore, regulation of melanoma cell growth, cell shapes and motility by Rac1 was also observed [54]. We used previously established culture of 1205Lu cells stably transfected with dominant negative Rac1N17 [62] in differentiation experiments. In the present study we observed substantial suppression of neurite growth in these melanoma cells after transfer to differentiation media (Fig. 9d, e).

In contrast to the neuronal pathway of trans-differentiation for 1205Lu and OM431 cells, HHMSX melanoma maintained compact adherent spheroid structures in differentiation media without apparent neurite growth, but with increasing expression of CD133, a cancer stem cell marker (Suppl. Figure 5b–d). A375 cells also survived in serum-free media with insulin, but exhibited a restricted ability for trans-differentiation (Suppl. Figure 5f).

Discussion

During embryonic development, melanoblasts, the precursors of melanocytes, emerge from a subpopulation of the neural crest stem/progenitor cells (which give also rise to the peripheral nervous system and several non-neural cell types) and migrate along a dorsolateral pathway to colonize skin. Melanoblasts populate the skin epidermis and further differentiate into melanocytes. Continuous melanocyte production in animal skin is dependent on the activity of the self-renewing melanoblasts (also known as melanocyte stem cells or regional neural crest stem cells) and of their differentiation into melanocytes. Melanoblasts are preferentially localized in the hair follicles of animal skin [63]. In human skin, where hair follicles are relatively sparse, melanoblasts also reside in the basal level of the interfollicular epidermis [64]. A rate of melanocyte proliferation was substantially downregulated in the process of differentiation: terminally differentiated melanocytes are long-living cells with rare cell divisions (one every 143 days) [20]. On the other hand, melanoblasts, maintain multipotency: under specific conditions they can differentiate not only into melanocytes but also into neurons and glial cells [42]. Interestingly, a recent study demonstrates direct conversion of human fibroblasts to functional melanocytes by a combination of over-expressed transcription factors, MITF, SOX10 and PAX3 [65].

Melanomas originate through somatic mutagenesis and epigenetic regulation during melanoblast differentiation into melanocytes and from young, actively proliferating melanocytes [37, 66]. Transcription factor MITF plays a central role in the terminal differentiation of melanocytes through a positive control of the tyrosinase gene expression and melanin production [67] and through a suppressive role for genes controlling stemness, OCT4 and NANOG [68]. The characteristic features of melanoma lines used in the current study, which were established from different phases of tumor development, demonstrated both differences and certain similarities. We observed average to high levels of the expression of SOX2 and NANOG, master pluripotency regulators, in all melanoma lines used in this study. A recent publication highlighted the critical role of SOX2 in regulation of self-renewal and tumorigenicity of human melanoma-initiating cells [69]. On the other hand, Nestin, an early neuroprogenitor marker, was almost completely absent in radial growth phase WM35 melanoma cells and in 60 % of a population of WM793 vertical growth phase melanoma cells, but was detected in all metastatic melanoma lines used in this study. SOX2 and Nestin coexpression was previously discovered in numerous samples of metastatic melanomas [70]. Taken together, our data highlighted well pronounced match of expression patterns

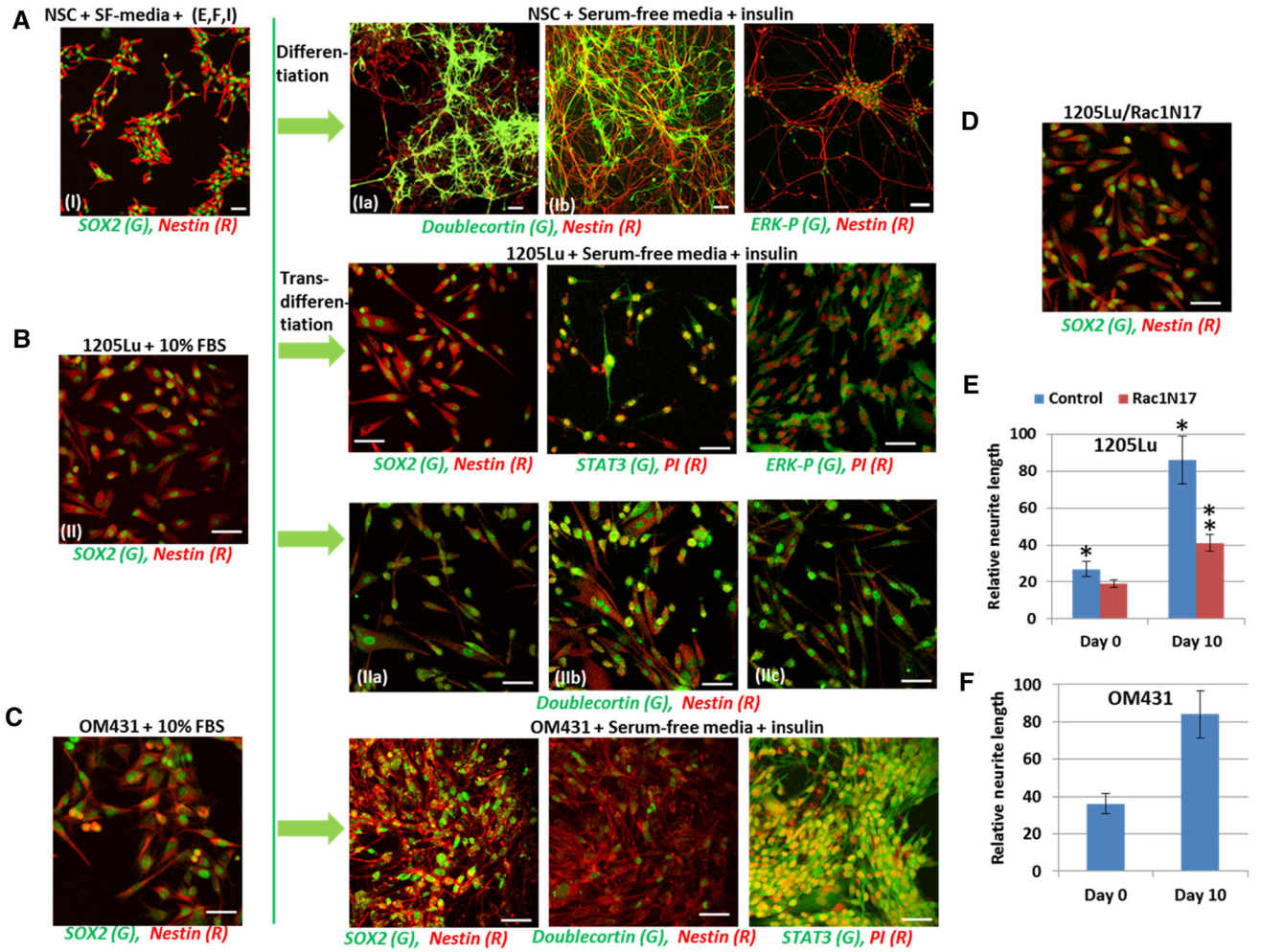

Fig. 9 **a** Neuronal differentiation of NSC (10 days) in serum-free differentiation media supplemented with B27 that contains insulin (5 μg/ml). **b** and **c** Neuronal pathway of differentiation of 1205Lu and OM431 melanoma cells (10 days) in the differentiation media with the B27 supplement. Confocal images were developed after immunostaining using rabbit polyclonal Ab to SOX2, a pluriopotency marker (*green*) and monoclonal antibody to Nestin, an early neuroprogenitor marker; polyclonal Ab to doublecortin, a neuronal marker (*green*) and monoclonal Ab to Nestin (*red*); polyclonal Ab to phospho-ERK (*green*) and PI, polyclonal Ab to STAT3 (*green*) and PI (*red*). *Bar* = 50 μm. Images from independent experiments: (I), (Ia) and (Ib); (IIIa), (IIIb) and (IIIc). **d** 1205Lu cells, which were stably transfected with dominant-negative Rac1N17, after 10 days in differentiation media. **e** and **f** Relative length of Nestin-containing neurites before (day 0) and 10 days after differentiation was determined using 5 random areas of images. *Error bars* represent mean ± SD ($p < 0.05$, Student's t test). *Stars* indicate significant difference in relative neurite length for normal 1205Lu cells at days 0 and 10; *double star* indicates significant difference between control and Rac1N17-transfected 1205Lu cells at day 10

of biomarkers in melanoma cells and in NSC. Comparable expression levels of FAS and DR5 for NSC and some melanoma lines underlined this similarity. In contrast, an additional stem cell marker CD166/ALCAM was not detectable in NSC, melanocytes, WM35 RGF and FEMX low metastatic melanoma cells, but was strongly expressed in A375 melanoma cells, emphasizing CD166 linkage with melanoma progression [32].

On the other hand, surface expression of NGFR, a potential marker of melanoma initiating cells [28], was found at low levels (NSC; WM35 and FEMX), intermediate levels (A375 and OM431) and high levels (WM793, 1235Lu and WM9). Interestingly, intracellular protein expression of NGFR was very high in WM35, A375, OM431 and HHMSX cells. CD133 surface expression was found at high levels only in NSC, at intermediate to low levels in FEMX and 1205Lu and at very low levels in WM35, WM793, A375, OM431 and HHMSX cells. CD133 total protein expression was also substantially higher than surface expression in WM35, WM9, WM793, FEMX, A375, OM431 and HHMSX cells, suggesting regulation of protein trafficking of receptors in these cells. Indeed, a role of FAP-1 for negative regulation of FAS receptor surface expression is well known [71, 72]. It is likely that a similar

mechanism can regulate NGFR surface expression, due to a similar NGFR/FAP-1 intracellular interaction [73].

Many investigations including our previous study demonstrated enrichment of a spheroid culture of glioblastoma U87MG by cancer stem cells after several passages [51, 59]. A similar approach was used for the isolation of a tumorigenic subpopulation with stem cell properties in melanoma, which also exhibited the ability for mesenchymal differentiation [47]. We observed relatively low CD133 expression on the cell surface of melanoma spheroids, which was modestly increased only in the HHMSX spheroid culture. The absence of enrichment of CD133 and CD20 biomarker expression in melanoma spheroid cultures was highlighted in a previously published paper [74]. Recently OCT4 overexpression driven by lentiviral OCT4 was used for infection of WM35 cells resulting in their dedifferentiation, which was associated with cancer stem cell phenotypes including significant increase of expression levels of endogenous NANOG and KLF4, as well as stem cell biomarkers, NGFR and ABCB5, but not CD133. Increased tumorigenicity of WM35-OCT4 cells was also observed [75]. In the current study we have not targeted identification of new biomarkers for melanoma cells; instead we have highlighted a differential ability of distinct melanoma lines to grow as spheroid cultures.

The central question of this study is regarding the plasticity of the neuronal pathway of trans-differentiation in melanoma. We did not observed dedifferentiation of metastatic melanoma cells via overexpression of the pluripotency factors and the subsequent induction of a new differentiation program. Instead, we observed a massive trans-differentiation along the neuronal pathway in the metastatic melanoma cells, 1235Lu and OM431, in the restricted culture conditions. The clinical cases of malignant melanomas with neural differentiation were previously observed [76, 77]. In contrast, HHMSX cells demonstrated cell survival, increased total protein expression of CD133, a marker for cancer stem cells, and the absence of neural differentiation after culturing in serum-free media supplemented with insulin. Furthermore, several melanoma lines, including WM793, died in these conditions, probably due to non-balanced autophagy followed by necrosis. In this respect, it was interesting to compare the resistant 1205Lu cells and the sensitive WM793 cells. A recent publication has demonstrated significant levels of the protective autophagy in metastatic 1205Lu cells, compared to the parent primary WM793 cells [78].

One of the aims of the present study was to further investigate the apoptotic and necroptotic death signaling events among melanoma cell lines from different stage of tumor progression. Similar to NSC, FEMX melanoma cells with high RIP1 kinase levels and total TNFR1 levels responded by development of both necroptosis and apoptosis after TNF+CHX treatment, while WM793 cells demonstrated a proapoptotic commitment, which was also observed among other melanoma lines, excluding HHMSX. Taken together, our results reveal that necroptosis could be induced at substantial levels in two melanoma lines, FEMX and OM431, while, in general, the mitochondrial pathway of apoptosis is prevalent in melanomas. Involvement of necroptotic signaling in induction of cell death, at least in some melanoma lines, may constitute a possibility for regulation of death in these resistant to treatment cancer cells.

In summary, all melanoma lines used in the current study express well pronounced levels of pluripotency markers, SOX2 and NANOG. There was a trend for increasing expression of the early neuroprogenitor marker-Nestin, during melanoma progression. Most of melanoma lines, especially WM35, FEMX and A375, could grow as spheroid cultures in serum-free media with supplements, similar to NSC. Such growth, beside well-known increase in tumorigenicity, was accompanied by significant down-regulation of surface expression levels of FAS, DR5 and NGFR1 and the corresponding decrease in death levels after signaling via FAS and DR5. Finally, it was possible to induce neural trans-differentiation of 1205Lu and OM431 cells confirmed by the expression of neuronal markers, doublecortin and β3-Tubulin, and by intensive neurite growth directed by RAC1. These data indicate a relative plasticity of differentiated melanoma cells and the possibility for their trans-differentiation without ectopic overexpression of OCT4 and OCT4-induced dedifferentiation. In conclusion, we observed four types of response of melanoma cells to restricted culturing conditions (serum-free serum + insulin): (i) cancer cell death probably via destructive autophagy (WM793) [78], (ii) maintenance of cancer cell stable differentiation (A375) or (iii) trans-differentiation (1205Lu), and (iv) cancer cell survival with increased proportions of the stem cell subpopulation (HHMSX). As a result of such trans-differentiation melanoma cells can acquire some characteristic features of young neurons and neuroblastoma cells. We hypothesized that the ability to differentiate for 1205Lu and OM431 cells was correlated with the maintenance of sensitivity to the induction of cell death; in contrast, the maintenance of the spheroid phenotype by HHMSX cells was linked with their resistance to cell death.

Materials and methods

Reagents

Fibronectin, laminin and polyornithine were obtained from Sigma-Aldrich (St. Louis, MO, USA). PI3 K inhibitor

LY294002, IKK inhibitor BMS345541, MAPK p38 inhibitor SB203580, and pan-caspase inhibitor zVAD-fmk were purchased from Calbiochem (La Jolla, CA, USA). Human soluble Killer-TRAIL (recombinant), Fas-Ligand (recombinant), anti-human TRAIL and anti-human Fas-Ligand antibodies were purchased from Alexis (San Diego, CA, USA); human TNFα, IL6 and IL8 were obtained from R&D Systems (Minneapolis, MN, USA).

Human embryonic neural stem cells (NSC)

Cryopreserved human embryonic neural stem cells (NSC) were obtained from Gibco/Life Technologies (Carlsbad, CA, USA) as a commercially available product (N7800-200). The cells were derived from NIH approved H9 (WA09) human embryonic stem cells. The cells were plated in 6-well culture plates coated with fibronectin and incubated at 37 °C in complete growth medium NSC/SFM, which contained serum-free DMEM/F12 supplemented with 2 mM GlutaMAX, bFGF (20 ng/ml), EGF (20 ng/ml) and StemPRO neural supplement (2 %). All reagents were obtained from Gibco/Life Technologies (Carlsbad, CA, USA).

Neuronal differentiation of human neural stem cells in culture

Neural stem cells were plated on polyornithine- and laminin-coated 6-well plates, which contained similarly coated cover slips, in complete NSC/SFM. After 2 days, neuronal differentiation was initiated by neuronal differentiation media, which contains Neurobasal medium, B-27 Serum-free supplement (2 %) and 2 mM GlutaMAX (Gibco/Life Technologies). Medium was changed every two days. A neuronal phenotype was confirmed using immunofluorescence detection 6-10 days after initiation of differentiation.

U87MG glioblastoma cells

Human glioblastoma (U87MG or HTB-14, ATCC) cell line was obtained from ATCC (Manassas, VA, USA). Cells were cultured in DMEM supplemented with 10 % FBS and 1 % pyruvate. For neurosphere formation, U87MG glioblastoma cells were cultured in the serum-free media DMEM/F12 supplemented with 2 mM GlutaMAX, bFGF (20 ng/ml), EGF (20 ng/ml) and B27 supplement (2 %). All reagents were obtained from from Gibco/Life Technologies (Carlsbad, CA, USA). After 15-20 passages, spheroid U87MG culture was significantly enriched by $CD133^+$ cells. For immunocytochemical analysis U87MG spheroids were attached to fibronectin matrix.

Human melanoma cells

Human melanoma cell lines 1205Lu, WM9, WM35, WM793 [38], FEMX, HHMSX [39], OM431 and A375 were maintained in DMEM medium supplemented with 10 % fetal bovine serum, L-glutamine and antibiotics. Cells were grown at 37 °C with 5 % CO_2. A375 cell line was obtained from American Type Culture Collection (ATCC, Manassas, VA, USA). For spheroid formation, melanoma cells were plated in 6-well culture plates and incubated at 37 °C in complete growth medium NSC/SFM, which contained serum-free DMEM/F12 supplemented with 2 mM GlutaMAX, bFGF (20 ng/ml), EGF (20 ng/ml) and StemPRO neural supplement (2 %) that also included insulin (5 μg/ml). All reagents were obtained from from Gibco/Life Technologies (Carlsbad, CA, USA). For induction of neuronal pathway of differentiation, melanoma cells were cultured in differentiation media as described above for neuronal differentiation of neural stem cells.

Immunocytochemistry analysis

Cells were fixed with 4 % paraformaldehyde in PBS for 20 min. Immunochemical staining was performed using standard protocols. Cells were stained for the undifferentiated NSC marker, Nestin (using mAb from Millipore, Temecula, CA, USA), and for the neuronal markers, doublecortin and beta3-Tubulin, using Abs from Cell Signaling (Danvers, MA, USA). Additional Abs against biomarkers include: SOX2, GFAP, STAT3, phospho-ERK (Cell Signaling), CD133 (Miltenyi Biotec, Auburn, CA) and COX2 (Cayman Chemical, Ann Arbor, MI). The secondary Abs were Alexa Fluor 594 goat anti-mouse IgG and Alexa Fluor 488 goat anti-rabbit IgG from Molecular Probes/Life Technologies (Carlsbad, CA, USA). A laser scanning confocal microscope (Nikon TE 2000 with EZ-C1 software, Tokyo, Japan) was used for immunofluorescence imaging.

FACS analysis of surface and total levels of cell receptors

Surface levels of NGFR, TRAIL-R2/DR5, FAS, TNFR1, TNFR2, CD133 and CD166 on human cell lines were determined by staining with a PE-conjugated Abs to the corresponding human proteins (R&D System, Minneapolis, MN, USA; eBioscience, San Diego, CA, USA; and Miltenyi Biotec, Auburn, CA, USA) and subsequently by use of flow cytometry. For detection of total levels of antigen proteins, cells were fixed and permeabilized using 0.5 % NP40 in PBS. PE-conjugated nonspecific mouse IgG1 was used as an immunoglobulin isotype control. A FACS Calibur flow cytometer (Becton Dickinson, Mountain

View, CA, USA) and the CellQuest program were used to perform flow cytometric analysis. All experiments were independently repeated 3-5 times.

Cell death studies

For induction of apoptosis, cells were exposed to small molecule inhibitors of cell signaling pathways. Furthermore, apoptosis was induced by TRAIL, TNFα, FasL and CHX alone or in combination. Apoptosis levels were then assessed by propidium iodide (PI) staining and quantifying the percentage of hypodiploid nuclei (pre-G1) using FACS analysis or by quantifying the percentage of Annexin-V-FITC-positive and PI-positive cells (BD Pharmingen, San Diego, CA), performed on a FACS Calibur flow cytometer (Becton Dickinson) using the CellQuest program. Trypan blue exclusion test was used for determination of cell viability and total death levels. Pan-caspase inhibitor, zVAD-fmk (40 μM) and RIP1 kinase inhibitor, Necrostatin-1 (40 μM), were added to cell cultures 1 h before induction of death signaling.

Western blot analysis

Total cell lysates (50 μg protein) were resolved on SDS-PAGE, and processed according to standard protocols. The monoclonal antibodies used for Western blotting included: anti-β-Actin (Sigma, St. Louis, MO, USA); anti-caspase-3 (Cell Signaling, Danvers, MA, USA). The polyclonal antibodies used included anti-phospho-p44/p42 MAP kinase (T202/Y204) and anti-p44/p42 MAP kinase; anti-phospho-JNK and anti-JNK1-3; anti-phospho-AKT (S473) and anti-AKT; anti-phospho-p65 (S536) NF-κB and anti-p65 NF-κB, anti-phospho-STAT3 (Y705) and anti-STAT3; anti-p53, anti-SOX2, anti-NANOG, anti-caspase-9, anti-RIP1 and anti-PARP-1 (Cell Signaling, Danvers, MA, USA); anti-FAS, and anti-DR5/TRAIL-R2 (Alexis, San Diego, CA, USA).The secondary antibodies were conjugated to horseradish peroxidase; signals were detected using the ECL system (Thermo Scientific, Rockford, IL, USA).

ELISA for IL6, IL8, and TNFα detection in the media

The ELISA kits for detection of human cytokines were purchased from R&D System, Minneapolis, MN, USA and eBioscience, San Diego, CA, USA.

Statistical analysis

Data from four to five independent experiments were calculated as means and standard deviations. Comparisons of results between treated and control groups were made by the Students' *t* tests. A *p* value of 0.05 or less between groups was considered significant.

Acknowledgments We would like to thank Drs. Peter Grabham and Howard Lieberman for advice, critical reading of the manuscript and discussion. This work was supported by Pilot Grant of the Department of Dermatology, Columbia University (P30AR044531-11, Project GG006336) and NIH Grant 5R01-ES12888-07.

Conflict of interest The authors declare that there are no conflicts of interest.

Compliance with Ethical Standards Animals were not used in this research. Participation of human subjects did not occur in this study.

References

1. Davies H, Bignell GR, Cox C, Stephens P, Edkins S, Clegg S, Teague J, Woffendin H, Garnett MJ, Bottomley W, Davis N, Dicks E, Ewing R, Floyd Y, Gray K, Hall S, Hawes R, Hughes J, Kosmidou V, Menzies A, Mould C, Parker A, Stevens C, Watt S, Hooper S, Wilson R, Jayatilake H, Gusterson BA, Cooper C, Shipley J, Hargrave D, Pritchard-Jones K, Maitland N, Chenevix-Trench G, Riggins GJ, Bigner DD, Palmieri G, Cossu A, Flanagan A, Nicholson A, Ho JW, Leung SY, Yuen ST, Weber BL, Seigler HF, Darrow TL, Paterson H, Marais R, Marshall CJ, Wooster R, Stratton MR, Futreal PA (2002) Mutations of the BRAF gene in human cancer. Nature 417:949–954
2. Pollock PM, Harper UL, Hansen KS, Yudt LM, Stark M, Robbins CM, Moses TY, Hostetter G, Wagner U, Kakareka J, Salem G, Pohida T, Heenan P, Duray P, Kallioniemi O, Hayward NK, Trent JM, Meltzer PS (2003) High frequency of BRAF mutations in nevi. Nat Genet 33:19–20. doi:10.1038/ng1054
3. Tsao H, Goel V, Wu H, Yang G, Haluska FG (2004) Genetic interaction between NRAS and BRAF mutations and PTEN/MMAC1 inactivation in melanoma. J Invest Dermatol 122:337–341. doi:10.1046/j.0022-202X.2004.22243.x
4. Curtin JA, Fridlyand J, Kageshita T, Patel HN, Busam KJ, Kutzner H, Cho KH, Aiba S, Brocker EB, LeBoit PE, Pinkel D, Bastian BC (2005) Distinct sets of genetic alterations in melanoma. N Engl J Med 353:2135–2147. doi:10.1056/NEJMoa050092
5. Tsao H, Zhang X, Fowlkes K, Haluska FG (2000) Relative reciprocity of NRAS and PTEN/MMAC1 alterations in cutaneous melanoma cell lines. Cancer Res 60:1800–1804
6. Hodis E, Watson IR, Kryukov GV, Arold ST, Imielinski M, Theurillat JP, Nickerson E, Auclair D, Li L, Place C, Dicara D, Ramos AH, Lawrence MS, Cibulskis K, Sivachenko A, Voet D, Saksena G, Stransky N, Onofrio RC, Winckler W, Ardlie K, Wagle N, Wargo J, Chong K, Morton DL, Stemke-Hale K, Chen G, Noble M, Meyerson M, Ladbury JE, Davies MA, Gershenwald JE, Wagner SN, Hoon DS, Schadendorf D, Lander ES, Gabriel SB, Getz G, Garraway LA, Chin L (2012) A landscape of driver mutations in melanoma. Cell 150:251–263. doi:10.1016/j.cell.2012.06.024
7. Vultur A, Villanueva J, Herlyn M (2011) Targeting BRAF in Advanced Melanoma: a First Step toward Manageable Disease. Clin Cancer Res 17:1658–1663. doi:10.1158/1078-0432.ccr-10-0174
8. Lipson EJ, Drake CG (2011) Ipilimumab: an anti-CTLA-4 antibody for metastatic melanoma. Clin Cancer Res 17:6958–6962. doi:10.1158/1078-0432.CCR-11-1595

9. Wolchok JD, Kluger H, Callahan MK, Postow MA, Rizvi NA, Lesokhin AM, Segal NH, Ariyan CE, Gordon RA, Reed K, Burke MM, Caldwell A, Kronenberg SA, Agunwamba BU, Zhang X, Lowy I, Inzunza HD, Feely W, Horak CE, Hong Q, Korman AJ, Wigginton JM, Gupta A, Sznol M (2013) Nivolumab plus ipilimumab in advanced melanoma. N Engl J Med 369:122–133. doi:10.1056/NEJMoa1302369
10. Chapman PB, Hauschild A, Robert C, Haanen JB, Ascierto P, Larkin J, Dummer R, Garbe C, Testori A, Maio M, Hogg D, Lorigan P, Lebbe C, Jouary T, Schadendorf D, Ribas A, O'Day SJ, Sosman JA, Kirkwood JM, Eggermont AM, Dreno B, Nolop K, Li J, Nelson B, Hou J, Lee RJ, Flaherty KT, McArthur AG (2011) Improved survival with vemurafenib in melanoma with BRAF V600E mutation. N Engl J Med 364:2507–2516. doi:10.1056/NEJMoa1103782
11. Flaherty KT, Puzanov I, Kim KB, Ribas A, McArthur GA, Sosman JA, O'Dwyer PJ, Lee RJ, Grippo JF, Nolop K, Chapman PB (2010) Inhibition of mutated, activated BRAF in metastatic melanoma. N Engl J Med 363:809–819. doi:10.1056/NEJMoa1002011
12. Nowell PC (1976) The clonal evolution of tumor cell populations. Science 194:23–28
13. Hanahan D, Weinberg RA (2011) Hallmarks of cancer: the next generation. Cell 144:646–674. doi:10.1016/j.cell.2011.02.013
14. Heidorn SJ, Milagre C, Whittaker S, Nourry A, Niculescu-Duvas I, Dhomen N, Hussain J, Reis-Filho JS, Springer CJ, Pritchard C, Marais R (2010) Kinase-dead BRAF and oncogenic RAS cooperate to drive tumor progression through CRAF. Cell 140:209–221. doi:10.1016/j.cell.2009.12.040
15. Vultur A, Villanueva J, Krepler C, Rajan G, Chen Q, Xiao M, Li L, Gimotty PA, Wilson M, Hayden J, Keeney F, Nathanson KL, Herlyn M (2014) MEK inhibition affects STAT3 signaling and invasion in human melanoma cell lines. Oncogene 33:1850–1861. doi:10.1038/onc.2013.131
16. Krasilnikov M, Ivanov VN, Dong J, Ronai Z (2003) ERK and PI3 K negatively regulate STAT-transcriptional activities in human melanoma cells: implications towards sensitization to apoptosis. Oncogene 22:4092–4101
17. Watson IR, Li L, Cabeceiras PK, Mahdavi M, Gutschner T, Genovese G, Wang G, Fang Z, Tepper JM, Stemke-Hale K, Tsai KY, Davies MA, Mills GB, Chin L (2014) The RAC1 P29S Hotspot Mutation in Melanoma Confers Resistance to Pharmacological Inhibition of RAF. Cancer Res 74:4845–4852. doi:10.1158/0008-5472.CAN-14-1232-T
18. Martz CA, Ottina KA, Singleton KR, Singleton KR, Jasper JS, Wardell SE, Peraza-Penton A, Anderson GR, Winter PS, Wang T, Alley HM, Kwong LN, Cooper ZA, Tetzlaff M, Chen PL, Rathmell JC, Flaherty KT, Wargo JA, McDonnell DP, Sabatini DM, Wood KC (2014) Systematic identification of signaling pathways with potential to confer anticancer drug resistance. Sci Signal 7:ra121. doi:10.1126/scisignal.aaa1877
19. Held MA, Langdon CG, Platt JT, Graham-Steed T, Liu Z, Chakraborty A, Bacchiocchi A, Koo A, Haskins JW, Bosenberg MW, Stern DF (2013) Genotype-selective combination therapies for melanoma identified by high-throughput drug screening. Cancer Discov 3:52–67. doi:10.1158/2159-8290.CD-12-0408
20. Tomasetti C, Vogelstein B (2015) Cancer etiology. Variation in cancer risk among tissues can be explained by the number of stem cell divisions. Science 347:78–81. doi:10.1126/science.1260825
21. Visvader JE, Lindeman GJ (2008) Cancer stem cells in solid tumours: accumulating evidence and unresolved questions. Nat Rev Cancer 8:755–768. doi:10.1038/nrc2499
22. Magee JA, Piskounova E, Morrison SJ (2012) Cancer stem cells: impact, heterogeneity, and uncertainty. Cancer Cell 21:283–296. doi:10.1016/j.ccr.2012.03.003
23. Kreso A, Dick JE (2014) Evolution of the cancer stem cell model. Cell Stem Cell 14:275–291. doi:10.1016/j.stem.2014.02.006
24. Smalley KS, Herlyn M (2009) Integrating tumor-initiating cells into the paradigm for melanoma targeted therapy. Int J Cancer 124:1245–1250. doi:10.1002/ijc.24129
25. Schatton T, Murphy GF, Frank NY, Yamaura K, Waaga-Gasser AM, Gasser M, Zhan Q, Jordan S, Duncan LM, Weishaupt C, Fuhlbrigge RC, Kupper TS, Sayegh MH, Frank MH (2008) Identification of cells initiating human melanomas. Nature 451:345–349. doi:10.1038/nature06489
26. Quintana E, Shackleton M, Sabel MS, Fullen DR, Johnson TM, Morrison SJ (2008) Efficient tumour formation by single human melanoma cells. Nature 456:593–598. doi:10.1038/nature07567
27. Held MA, Curley DP, Dankort D, McMahon M, Muthusamy V, Bosenberg MW (2010) Characterization of melanoma cells capable of propagating tumors from a single cell. Cancer Res 70:388–397. doi:10.1158/0008-5472.CAN-09-2153
28. Boiko AD, Razorenova OV, van de Rijn M, Swetter SM, Johnson DL, Ly DP, Butler PD, Yang GP, Joshua B, Kaplan MJ, Longaker MT, Weissman IL (2010) Human melanoma-initiating cells express neural crest nerve growth factor receptor CD271. Nature 466:133–137. doi:10.1038/nature09161
29. Lang D, Mascarenhas JB, Shea CR (2013) Melanocytes, melanocyte stem cells, and melanoma stem cells. Clin Dermatol 31:166–178. doi:10.1016/j.clindermatol.2012.08.014
30. Murphy GF, Wilson BJ, Girouard SD, Frank NY, Frank MH (2014) Stem cells and targeted approaches to melanoma cure. Molecular Asp Med 39C:33–49. doi:10.1016/j.mam.2013.10.003
31. Redmer T, Welte Y, Behrens D, Fichtner I, Przybilla D, Wruck W, Yaspo ML, Lehrach H, Schafer R, Regenbrecht CR (2014) The nerve growth factor receptor CD271 is crucial to maintain tumorigenicity and stem-like properties of melanoma cells. PLoS ONE 9:e92596. doi:10.1371/journal.pone.0092596
32. Klein WM, Wu BP, Zhao S, Wu H, Klein-Szanto AJ, Tahan SR (2007) Increased expression of stem cell markers in malignant melanoma. Mod Pathol 20:102–107. doi:10.1038/modpathol.3800720
33. Ashkenazi A, Herbst RS (2008) To kill a tumor cell: the potential of proapoptotic receptor agonists. J Clin Invest 118:1979–1990
34. Jin Z, El-Deiry WS (2005) Overview of cell death signaling pathways. Cancer Biol Ther 4:139–163
35. Degterev A, Hitomi J, Germscheid M, Ch'en IL, Korkina O, Teng X, Abbott D, Cuny GD, Yuan C, Wagner G, Hedrick SM, Gerber SA, Lugovskoy A, Yuan J (2008) Identification of RIP1 kinase as a specific cellular target of necrostatins. Nat Chem Biol 4:313–321. doi:10.1038/nchembio.83
36. Vandenabeele P, Galluzzi L, Vanden Berghe T, Kroemer G (2010) Molecular mechanisms of necroptosis: an ordered cellular explosion. Nat Rev Mol Cell Biol 11:700–714. doi:10.1038/nrm2970
37. Vultur A, Herlyn M (2013) SnapShot: melanoma. Cancer Cell 23(706–706):e701. doi:10.1016/j.ccr.2013.05.001
38. Satyamoorthy K, DeJesus E, Linnenbach AJ, Kraj B, Kornreich DL, Rendle S, Elder DE, Herlyn M (1997) Melanoma cell lines from different stages of progression and their biological and molecular analyses. Melanoma Res 7(Suppl 2):S35–42
39. Myklebust AT, Helseth A, Breistol K, Hall WA, Fodstad O (1994) Nude rat models for human tumor metastasis to CNS. Procedures for intracarotid delivery of cancer cells and drugs. J Neurooncol 21:215–224
40. Haass NK, Sproesser K, Nguyen TK, Contractor R, Medina CA, Nathanson KL, Herlyn M, Smalley KS (2008) The mitogen-activated protein/extracellular signal-regulated kinase kinase inhibitor AZD6244 (ARRY-142886) induces growth arrest in melanoma cells and tumor regression when combined with

docetaxel. Clin Cancer Res 14:230–239. doi:10.1158/1078-0432.CCR-07-1440
41. Peter ME, Legembre P, Barnhart BC (2005) Does CD95 have tumor promoting activities? Biochim Biophys Acta 1755:25–36
42. Kunisada T, Tezulka K, Aoki H, Motohashi T (2014) The stemness of neural crest cells and their derivatives. Birth Defects Res Part C 102:251–262. doi:10.1002/bdrc.21079
43. Juhasz I, Albelda SM, Elder DE, Murphy GF, Adachi K, Herlyn D, Valyi-Nagy IT, Herlyn M (1993) Growth and invasion of human melanomas in human skin grafted to immunodeficient mice. Am J Pathol 143:528–537
44. Satyamoorthy K, Li G, Gerrero MR, Brose MS, Volpe P, Weber BL, Van Belle P, Elder DE, Herlyn M (2003) Constitutive mitogen-activated protein kinase activation in melanoma is mediated by both BRAF mutations and autocrine growth factor stimulation. Cancer Res 63:756–759
45. Tamada K, Chen L (2006) Renewed interest in cancer immunotherapy with the tumor necrosis factor superfamily molecules. Cancer Immunol Immunother 55:355–362. doi:10.1007/s00262-005-0081-y
46. Ivanov VN, Hei TK (2014) A role for TRAIL/TRAIL-R2 in radiation-induced apoptosis and radiation-induced bystander response of human neural stem cells. Apoptosis 19:399–413. doi:10.1007/s10495-013-0925-4
47. Fang D, Nguyen TK, Leishear K, Finko R, Kulp AN, Hotz S, Van Belle PA, Xu X, Elder DE, Herlyn M (2005) A tumorigenic subpopulation with stem cell properties in melanomas. Cancer Res 65:9328–9337. doi:10.1158/0008-5472.CAN-05-1343
48. Karin M (2009) NF-kappaB as a critical link between inflammation and cancer. Cold Spring Harb Perspect Biol 1:a000141. doi:10.1101/cshperspect.a000141
49. Franke TF (2008) PI3 K/Akt: getting it right matters. Oncogene 27:6473–6488. doi:10.1038/onc.2008.313
50. Grivennikov SI, Greten FR, Karin M (2010) Immunity, inflammation, and cancer. Cell 140:883–899. doi:10.1016/j.cell.2010.01.025
51. Ivanov VN, Hei TK (2014) Radiation-induced glioblastoma signaling cascade regulates viability, apoptosis and differentiation of neural stem cells (NSC). Apoptosis 19:1736–1754. doi:10.1007/s10495-014-1040-x
52. Grivennikov S, Karin M (2008) Autocrine IL-6 signaling: a key event in tumorigenesis? Cancer Cell 13:7–9
53. Ivanov VN, Hei TK (2004) Arsenite sensitizes human melanomas to apoptosis via tumor necrosis factor alpha-mediated pathway. J Biol Chem 279:22747–22758
54. Bauer NN, Chen YW, Samant RS, Shevde LA, Fodstad O (2007) Rac1 activity regulates proliferation of aggressive metastatic melanoma. Exp Cell Res 313:3832–3839. doi:10.1016/j.yexcr.2007.08.017
55. Chun KS, Surh YJ (2004) Signal transduction pathways regulating cyclooxygenase-2 expression: potential molecular targets for chemoprevention. Biochem Pharmacol 68:1089–1100
56. Ivanov VN, Partridge MA, Huang SX, Hei TK (2011) Suppression of the proinflammatory response of metastatic melanoma cells increases TRAIL-induced apoptosis. J Cell Biochem 112:463–475. doi:10.1002/jcb.22934
57. Denkert C, Kobel M, Berger S, Siegert A, Leclere A, Trefzer U, Hauptmann S (2001) Expression of cyclooxygenase 2 in human malignant melanoma. Cancer Res 61:303–308
58. Lopez-Bergami P, Huang C, Goydos JS, Yip D, Bar-Eli M, Herlyn M, Smalley KS, Mahale A, Eroshkin A, Aaronson S, Ronai Z (2007) Rewired ERK-JNK signaling pathways in melanoma. Cancer Cell 11:447–460. doi:10.1016/j.ccr.2007.03.009
59. Hardee ME, Marciscano AE, Medina-Ramirez CM, Zagzag D, Narayana A, Lonning SM, Barcellos-Hoff MH (2012) Resistance of glioblastoma-initiating cells to radiation mediated by the tumor microenvironment can be abolished by inhibiting transforming growth factor-beta. Cancer Res 72:4119–4129. doi:10.1158/0008-5472.CAN-12-0546
60. Grabham PW, Reznik B, Goldberg DJ (2003) Microtubule and Rac 1-dependent F-actin in growth cones. J Cell Sci 116:3739–3748. doi:10.1242/jcs.00686
61. Vadodaria KC, Brakebusch C, Suter U, Jessberger S (2013) Stage-specific functions of the small Rho GTPases Cdc42 and Rac1 for adult hippocampal neurogenesis. J Neurosci 33:1179–1189. doi:10.1523/JNEUROSCI.2103-12.2013
62. Ivanov VN, Krasilnikov M, Ronai Z (2002) Regulation of Fas expression by STAT3 and c-Jun is mediated by phosphatidylinositol 3-kinase-AKT signaling. J Biol Chem 277:4932–4944
63. Nishimura EK (2011) Melanocyte stem cells: a melanocyte reservoir in hair follicles for hair and skin pigmentation. Pigment Cell Melanoma Res 24:401–410. doi:10.1111/j.1755-148X.2011.00855.x
64. Liu J, Fukunaga-Kalabis M, Li L, Herlyn M (2014) Developmental pathways activated in melanocytes and melanoma. Arch Biochem Biophys. doi:10.1016/j.abb.2014.07.023
65. Yang R, Zheng Y, Li L, Liu S, Burrows M, Wei Z, Nace A, Herlyn M, Cui R, Guo W, Cotsarelis G, Xu X (2014) Direct conversion of mouse and human fibroblasts to functional melanocytes by defined factors. Nat Commun 5:5807. doi:10.1038/ncomms6807
66. Uong A, Zon LI (2010) Melanocytes in development and cancer. J Cell Physiol 222:38–41. doi:10.1002/jcp.21935
67. Chin L, Garraway LA, Fisher DE (2006) Malignant melanoma: genetics and therapeutics in the genomic era. Genes Dev 20:2149–2182
68. Cheli Y, Giuliano S, Botton T, Rocchi S, Hofman V, Hofman P, Bahadoran P, Bertolotto C, Ballotti R (2011) Mitf is the key molecular switch between mouse or human melanoma initiating cells and their differentiated progeny. Oncogene 30:2307–2318. doi:10.1038/onc.2010.598
69. Santini R, Pietrobono S, Pandolfi S, Montagnani V, D'Amico M, Penachioni JY, Vinci MC, Borgognoni L, Stecca B (2014) SOX2 regulates self-renewal and tumorigenicity of human melanoma-initiating cells. Oncogene 33:4697–4708. doi:10.1038/onc.2014.71
70. Laga AC, Zhan Q, Weishaupt C, Ma J, Frank MH, Murphy GF (2011) SOX2 and nestin expression in human melanoma: an immunohistochemical and experimental study. Exp Dermatol 20:339–345. doi:10.1111/j.1600-0625.2011.01247.x
71. Ivanov VN, Lopez Bergami P, Maulit G, Sato TA, Sassoon D, Ronai Z (2003) FAP-1 association with Fas (Apo-1) inhibits Fas expression on the cell surface. Mol Cell Biol 23:3623–3635
72. Ivanov VN, Ronai Z, Hei TK (2006) Opposite roles of FAP-1 and dynamin in the regulation of Fas (CD95) translocation to the cell surface and susceptibility to Fas ligand-mediated apoptosis. J Biol Chem 281:1840–1852
73. Irie S, Hachiya T, Rabizadeh S, Maruyama W, Mukai J, Li Y, Reed JC, Bredesen DE, Sato TA (1999) Functional interaction of Fas-associated phosphatase-1 (FAP-1) with p75(NTR) and their effect on NF-kappaB activation. FEBS Lett 460:191–198
74. Ramgolam K, Lauriol J, Lalou C, Lauden L, Michel L, de la Grange P, Khatib AM, Aoudjit F, Charron D, Alcaide-Loridan C, Al-Daccak R (2011) Melanoma spheroids grown under neural crest cell conditions are highly plastic migratory/invasive tumor cells endowed with immunomodulator function. PLoS ONE 6:e18784. doi:10.1371/journal.pone.0018784
75. Kumar SM, Liu S, Lu H, Zhang H, Zhang PJ, Gimotty PA, Guerra M, Guo W, Xu X (2012) Acquired cancer stem cell phenotypes through Oct4-mediated dedifferentiation. Oncogene 31:4898–4911. doi:10.1038/onc.2011.656
76. Reed RJ, Leonard DD (1979) Neurotropic melanoma. A variant of desmoplastic melanoma. Am J Surg Pathol 3:301–311

77. Su A, Dry SM, Binder SW, Said J, Shintaku P, Sarantopoulos GP (2014) Malignant melanoma with neural differentiation: an exceptional case report and brief review of the pertinent literature. Am J Dermatopathol 36:e5–9. doi:10.1097/DAD.0b013e31828cf90a

78. Kraya AA, Piao S, Xu X, Zhang G, Herlyn M, Gimotty P, Levine B, Amaravadi RK, Speicher DW (2014) Identification of secreted proteins that reflect autophagy dynamics within tumor cells. Autophagy. doi:10.4161/15548627.2014.984273